Table 3
Pharmacogenetics of drug-metabolizing enzymes (non-P450)

Drug-metabolizing enzymes	Gene	Genotypes	Major allelic variants	Phenotypes: Frequency	
				Caucasian	Asian (Japanese)
Thiopurine *S*-methyltransferase	TPMT	*1–*15	*2, *3	EM: 73–89% IM: 11–27% PM: 0–4%	EM: 97% IM: 3%
Dihydropyrimidine dehydrogenase	DPYD	*1–*12	*2	EM: 97% PM: 3%	
N-acetyltransferase 2	NAT2	*4–*19	*5, *6, *7, *14	EM: 25% IM: 25% PM: 50%	EM: 45% IM: 45% PM: 10%
UDP-glucuronosyltransferase 1A1	UGT1A1	*1–*64	*6, *7, *27, *28, *29	EM: 90% PM: 10%	EM: 99% PM: 1%
Catechol O-methyltransferase	COMT		Val158Met	EM: 75% PM: 25%	
Glutathione *S*-transferase M1	GSTM1		null		
Glutathione *S*-transferase M3	GSTM3		*A, *B		
Glutathione *S*-transferase-P1	GSTP1		Ile105Val		
Glutathione *S*-transferase-T1	GSTT1		null		

EM=extensive metabolizer; IM=intermediate metabolizer; PM=poor metabolizer.

2.3. Non-enzymes

Recently, genetic polymorphisms, other than those for enzymes for drug metabolism, have drawn attention as important factors for drug responses. They include those for drug transporters, receptors, transport protein, and mitochondria DNA (mtDNA) (Table 4). Especially, the focus has been on genetic polymorphisms for receptors that can be the molecular target for drugs. An anti-lung cancer drug gefitinib binds the site for epidermal growth factor receptor-tyrosine kinase (EGFR-TK) and blocks the signal transduction for cancer proliferation. An individual variation in the effect of gefitinib was reported [29–31], and good response was observed in the patients with a polymorphism in the EGFR-TK domain. On the other hand, gefitinib was not effective in the patients without polymorphisms in the EGFR-TK domain.

3. Genotyping methods

Recent progress in genetic testing technologies is remarkable, and they are applied for the analysis of genetic mutations and polymorphisms that regulate disease vulnerability and drug responses. Classically, the PCR-RFLP analysis and the allele-specific amplification method had been used for the detection of SNP [32]. However, these methods require rather troublesome maneuvers such as electrophoresis after PCR and staining with ethidium bromide. A few years ago a new method was developed to cover the shortcomings of these genetic tests. The method is called real-time PCR because it uses a fluorescent probe or dye in the PCR reaction to detect DNA amounts and characteristic base compositions over time [33,34]. These methods allow the detection of SNP within about 40 min to 2 h of DNA extraction. For real-time PCR, the TaqMan probe and Hybridization probe methods are used in a number of institutes to detect various SNPs (Table 5).

3.1. Real-time PCR

3.1.1. TaqMan probe

The TaqMan probe method employs 5′-exonuclease activity of Taq DNA polymerase for PCR. The TaqMan probe consists of an oligo-nucleotide of about 20–30-mer and labeled with a reporter fluorescent dye at the 5′-terminus and a quencher fluorescent dye at the 3′-terminus. The two fluorescent dyes on the TaqMan probe are in a state of decreased fluorescent intensity due to fluorescence resonance energy transfer (FRET) phenomenon when they are close in physical distance. However, the 5′-exonuclease of Taq DNA polymerase cleaves the binding of the fluorescent dye along the extension reaction. The fluorescent dye is released from the influence of the quencher and fluoresces. In general, the TaqMan probe is designed to be at the center of SNP.

Recently, we developed a new real-time PCR method using allele-specific amplification [38]. We designed PCR primers at the site of SNP so that not only the TaqMan probe, but also less expensive SYBR Green I is available [38,54]. ABI PRISM7000, 7300, 7500, PRISM7700, 7900Fast (Applied Biosystems), LightCycler (Roche), Mx4000, Mx3000P (STRATAGENE), and Smart Cycler II (TaKaRa) can be used for detection.

3.1.2. Hybridization probe

The Hybridization Probe method allows real-time detection of PCR products and SNP using two fluorescent probes. Firstly, PCR primers are designed to amplify the target sequence including SNP. Secondly, a probe labeled with fluorescein at the 3′-terminus is designed so that it

Table 4
Genes associated with altered drug effect

Name	Gene	Drug
MDR1, *P*-glycoprotein	ABCB1	digoxin
Angiotensin converting enzyme	ACE	ACE inhibitors
β-1 adrenergic receptor	ADRB1	β adrenergic receptor antagonists
β-2 adrenergic receptor	ADRB2	albuterol, salbutamol
Angiotensinogen	AGT	antihypertensive drugs
Angiotensin-II receptor type1	AGTR1	angiotensin-II receptor antagonists
Arachidonate 5-lipoxygenase	ALOX5	5-lipoxygenase inhibtors, leukotriene receptor antagonists
Bradykinin receptor B2	BDKRB2	ACE inhibitors
Cholesteryl ester transfer protein	CETP	pravastatin, atorvastatin
Dopamine D2 receptor	DRD2	haloperidol, nemonapride
Dopamine D3 receptor	DRD3	clozapine
Dopamine D4 receptor	DRD4	neuroleptics
Epidermal growth factor receptor	EGFR	gefitinib, erlotinib
Guanine nucleotide-binding protein, B3 subunit	GNB3	antidepressants
N-methyl-D-aspartate receptor 2B subunit	GRIN2B	clozapine
5-hydroxytryptamine receptor 2A	HTR2A	antipsychotic drugs
Inositol polyphosphate 1-phosphatase	INPP1	lithium
Inosine triphosphate pyrophosphatase	ITPA	azathioprine
Hepatic lipase	LIPC	statins
Leukotriene C4 synthase	LTC4S	zafirlukast, pranlukast
Mitochondrial DNA	mtDNA	aminoglycoside antibiotics
5, 10-Methylenetetrahydrofolate reductase	MTHFR	methotrexate, 5-fluorourasil
Organic anion transporting polypeptide-C	OATP-C	pravastatin
Peroxisome-proliferator activated receptors alpha	PPARA	fenofibrate
Dopamine transporter	SLC6A3	methylphenidate
Serotonin transporter	SLC6A4	fluoxetine, paroxetine
Tryptophan hydroxylase 1	TPH1	antidepressants
Thymidylate synthase	TYMS	5-fluorourasil

can hybridize the sequence in the PCR product amplified with these primers. At the close site, another probe labeled with LCRed640 at the 5′-terminus and phosphate at the 3′-terminus is designed. They are designed so that SNP is located at the center of either one of these probes. SNP is detected by the analysis of the melting curve. In other words, temperature is raised slowly after PCR with fluorescent signals monitored. At a certain temperature, a probe with lower Tm dissociates and fluorescein is separated from LCRed640, and fluorescent intensity drastically plummets. In other words, a mismatch between the template and the probe allows dissociation more easily than the completely matched sequence, and as a result the presence or absence of SNP is detected. LightCycler (Roche) is required for the detection. Roche has already started the sales of mutation detection kits for CYP2C9 (*2 and *3), CYP2C19 (*2 and *3), and NAT2 (*5, *6, *7 and *14) on a commercial basis.

3.1.3. Other real-time PCR

HyBeacon Probe [55] and a real-time PCR method with a 3′-locked nucleic acid primer [56] have been reported for the detection of SNP. In addition, High-Resolution Melting Assay with a fluorescent dye LCGreen I [57,58], which can be incorporated into double-strand DNA in a saturated manner, has been developed to cover the shortcomings of SYBR Green I that was previously used. Other than PCR, for the amplification methods at the fixed temperature, loop-mediated isothermal amplification (LAMP) [59] and isothermal and chimeric primer-initiated amplification of nucleic acids (ICAN) (http://www.takara.co.jp/english/index.htm) have been developed. These gene amplification methods do not require an expensive thermalcycler and have the advantage that a less expensive block incubator can be used. However, designing primers is more troublesome than PCR and requires special software.

3.2. Other methods

As other genetic tests, Denaturing High Performance Liquid Chromatography (DHPLC) [60], Pyrosequencing [61], Invader assay [62,63], Luminex assay [64], Mass Array using Matrix-Assisted Laser Desorption Ionization Time of Flight Mass Spectrometry (MALDI-TOF-MS) [65], SNPstream [66], DNA Chip [67], Nano Chip [68], and eSensor chip [64] have been widely used in laboratories. Regarding DNA Chip, Roche has started sales of AmpliChip CYP450 on a commercial basis, which can detect CYP2D6 polymorphisms (http://www.roche-diagnostics.com/products_services/amplichip_cyp450.html).

3.3. Point-of-care testing

Currently, the TaqMan Assay, melting curve analysis, and direct sequencing are genetic testing technologies generally used in the laboratories. On the other hand, Pyrosequencing, TOF-MS, and DNA Chip, which require relatively expensive specific equipment and special techniques, are used in entrusted analysis institutes and genome centers. For the application of tailor-made drug therapy to clinical settings, point-of-care testing that allows easy genetic testing at the patient bedside and the clinic will be necessary in the future. We recently developed point-of-care genetic testing using immunochromatography [69,70]. In this method, the reaction after PCR is dropped on a strip and visual judgment of the SNP becomes possible by the appearance of a purple line on the strip when SNP is present. Detection requires 10 min after PCR and the method allows a simple and rapid genetic testing.

Table 5
Examples of pharmacogenetic markers detected by real-time PCR assay (TaqMan assay and Hybridization probe assay)

TaqMan assay	Hybridization probe assay
ADRB2 (46A>G) [35]	ADRB2 (46A>G) [43]
ADRB2 (79C>G) [35]	ADRB2 (79C>G) [43]
CETP (270C>T, B2 allele) [36]	CETP (270C>T, B2 allele) [43]
CYP2B6 (516G>T, *6,*7, *9 or *13 allele) [37]	CYP1A1 (4889A>G) [44]
CYP2C9 (416C>T, *2 allele) [38]	CYP1B1 (432C>G, *2 allele) [45]
CYP2C9 (1061A>C, *3 allele) [38]	CYP2C9 (416C>T, *2 allele) (www.roche-applied-science.com)
CYP2C19 (681G>A, *2 allele) [38]	CYP2C9 (1061A>C, *3 allele) (www.roche-applied-science.com)
CYP2C19 (636 G>A, *3 allele) [38]	CYP2C19 (681G>A, *2 allele) (www.roche-applied-science.com)
CYP2D6 (gene duplication, *2 × 2 allele) [39]	CYP2C19 (636 G>A, *3 allele) (www.roche-applied-science.com)
CYP2D6 (1846G>A, *4 allele) [38]	CYP2D6 (-1584 C>G, *2 allele) [46]
CYP2D6 (gene deletion, *5 allele) [39]	CYP2D6 (gene duplication, *2 × 2 allele) [46]
CYP2D6 (100C>T, *10 allele) [38]	CYP2D6 (gene deletion, *5 allele) [46]
CYP2D6 (1758G>A, *14 allele) [38]	CYP2D6 (31 G>A, *35 allele) [46]
CYP2D6 (4125–4133insGTGCCCACT, *18 allele) [38]	GSTM1 (gene deletion) [47]
CYP2D6 (2573insC, *21 allele) [38]	GSTT1 (gene deletion) [47]
CYP3A5 (6981A>G, *3 allele) [37,40]	GSTP1 (A>G, Ile105Val allele) [47]
CYP3A5 (14685A>G, *6 allele) [37]	HTR2A (102T>C) [43]
LTC4S (-444A>C) [41]	INPP1 (973C>A) [43]
MDR1 (-129T>C) [42]	MDR1 (3435C>T) [48]
MDR1 (325G>A) [42]	mtDNA (1555A>G) [43]
MDR1 (2677G>T/A) [42]	MTHFR (677C>T) [49,50]
MDR1 (3435C>T) [42]	NAT2 (341T>C, *5 allele) [51]
NAT2 (341T>C, *5 allele) [38]	NAT2 (481C>T, *5 allele) [52]
NAT2 (481C>T, *5 allele) [38]	NAT2 (590G>A, *6 allele) [52]
NAT2 (590G>A, *6 allele) [38]	NAT2 (857G>A, *7 allele) [52]
NAT2 (857G>A, *7 allele) [38]	NAT2 (191G>A, 14 allele) (www.roche-applied-science.com)
TPMT (719A>G, *3C) [38]	TPMT (238G>C, *2 allele) [53]
	TPMT (460G>A, 719A>G, *3A) [53]
	TPMT (460G>A, *3B) [53]
	TPMT (719A>G, *3C) [53]
	TPMT (292G>T, 460G>A, 719A>G, *3D) [53]
	TPMT (intron9/exon10 splice junction G>A, *4 allele) [53]
	TPMT (146T>C, *5 allele) [53]
	TPMT (539A>T, *6 allele) [53]
	TPMT (681T>G, *7 allele) [53]

4. Clinical application

There are a number of reports on the association of genetic polymorphisms involved in drug responses with pharmacodynamics, efficacy, and adverse effects, but few cases have been clinically applied. In particular, evidence that supports clinical application has been accumulated for NAT2, CYP2C19, TPMT, and mtDNA A1555G.

4.1. NAT2 genotyping for isoniazid treatment

Since NAT2 is involved in the acetylation of isoniazid, sulphamethazine, and procaine amide, blood concentrations of these drugs are expected to increase and result in higher incidences of adverse events in the SA for NAT2. Since rifampicin, often concomitantly administered with isoniazid for tuberculosis, induces an oxidative hydrolysis enzyme and the production of hydralazine, a toxic metabolite, it has been reported that the drug is likely to cause liver disorder in SA patients [24].

We conducted genetic testing for NAT2 by real-time PCR on 102 Japanese patients receiving isoniazid, without concomitant administration of rifampicin [71]. As a result, adverse events appeared in six patients in total and in 83.3% of the SA for NAT2. There were various adverse events such as nausea, vomiting, fever, visual disturbance, and peripheral nerve injury, and reduction or termination of isoniazid successfully decreased or eliminated adverse events in these patients. The adverse effects of isoniazid were not so critical, but genetic testing for NAT2 should be clinically applied so that the administration does not decrease the QOL of the patients.

4.2. CYP2C19 genotyping for omeprazole treatment

Proton pump inhibitors have a potent acid suppressive effect, and a combination with antibiotics is used to eradicate *Helicobacter pylori* (*H. pylori*) and treat ulcer in the upper gastrointestinal tract. Proton pump inhibitors are mainly metabolized by CYP2C19 and the pharmacodynamics and efficacy are influenced by the CYP2C19 polymorphism. Furuta et al. [72] found that the eradication rates of *H. pylori* with omeprazole 20 mg/day plus amoxicillin 2000 mg/day for 6 or 8 weeks were 28.6% in the EM, 60.0% in the IM, and 100.0% in the PM, and there was a significant difference among genetic polymorphisms. In the PM, the aforementioned doses of the two drugs, a proton pump inhibitor and amoxicillin, yielded a sufficient eradication rate, and the necessity to increase the dose of a proton pump inhibitor in the EM and the IM was verified clinically. Furthermore, CYP2C19 polymorphism affects treatment efficacy by the mainstream three-drug regimen. The eradication rates of *H. pylori* with omeprazole 40 mg/day or lansoprazole 60 mg/day, and amoxicillin 1500 mg/day and clarithromycin 600 mg/day for 1 week were 72.7% in the EM,

92.1% in the IM, and 97.8% in the PM [73]. The factors responsible for the eradication failure include the presence of clarithromycin-resistant *H. pylori* strains, and in the future it will be necessary to test not only CYP2C19 polymorphism, but also genotypes for clarithromycin resistance in *H. pylori*.

4.3. TPMT genotyping for 6-MP treatment

Phenotypes of TPMT activity are often evaluated by the less invasive measurement of the activity in the red blood cells of the patients. It was reported that 92% exhibited high activity while 7.7% showed intermediate activity, and 1 in 300 revealed no TPMT activity in Caucasians [74]. In Caucasian infant patients with acute myeloid leukemia, the concentrations of the active metabolite of 6-MP were significantly higher in the red blood cells in those carrying TPMT*2, *3A, *3B, or *3C alleles, and dose reduction or termination of the administration was required in all patients [21]. Evans et al. [75] reported that when 6-MP was administered at 500 mg/m^2/week in the EM for TPMT, the dose should be reduced to half in the IM and 20 mg/m^2/week or 1/25-fold in the PM. Indeed, the evaluated results of phenotypes and genotypes for TPMT were applied to determining doses of 6-MP to patients at St. Jude Children's Hospital.

4.4. mtDNA A1555G genotyping for aminoglycoside treatment

It has been reported that the administration of aminoglycoside antibiotics is likely to cause irreversible perceptive deafness in humans with the SNP at the 1555th base (A to G) in the 12S rRNA gene in mtDNA [76]. Aminoglycosides basically inhibit the synthesis of bacterial protein, but in cases with the alteration at the 1555th base from A to G in the mtDNA in normal humans, the sequence shares a similar three-dimensional structure with bacterial 16S rRNA, and the site that originally does not have the affinity becomes the target for aminoglycosides and protein synthesis involved in the mitochondrial electron transfer system and oxidative phosphorylation is suppressed. As a result, ATP production decreases and hair cells in the internal ear show dysfunction [77].

We performed genetic testing for mtDNA A1555G in patients with perceptive deafness using real-time PCR and point-of-care testing [70]. Recently, following the request by a patient (Mother) with perceptive deafness carrying the mtDNA A1555G alteration, we performed genetic testing for the same polymorphism in her children (a 13-year-old boy and an 11-year-old girl) without the symptom of perceptive deafness. As a result, both children carried the genotype of 1555G and were recommended to carry an adverse effect avoidance card reported by Usami et al. [78] so that aminoglycosides would not be given (personal communications). Perceptive deafness is irreversible and decreases the QOL of the patients remarkably. It is necessary to perform genetic testing routinely before aminoglycoside administration and promote counseling for mtDNA A1555G subjects to avoid side effects.

5. Cost effectiveness

Few reports have investigated the benefit for medical economy by testing the genes involved in drug responses prior to drug therapy. Tavadia et al. [79] calculated that on the assumption that azathioprine caused myelosuppression in 100% of the PM and 30% of the IM for TPMT, genetic testing would provide about $200 in cost benefit. Simulating eradication therapy in 100 cases with omeprazole and amoxicillin for 3 months according to the eradication regimen for *H. pylori* reported by Furata et al. [73], Desta et al. [80] calculated the cost per patient for the testing of CYP2C19 polymorphisms (*1, *2, and *3) with the conventional method in the laboratories and the drug cost for omeprazole, and concluded that genetic testing for CYP2C19 in advance could save Asians $5680 in medical costs.

6. Conclusions

Today it is possible to predict the responder and non-responder, and the emergence of adverse effects for some drugs by polymorphism testing of the genes involved in drug responses. However, there are markedly few institutes in the world where genetic testing is routinely performed and applied to tailor-made drug therapy. Recently, the Food and Drug Administration (FDA) in the US declared guidance on using individual information on genetic polymorphisms in the approval of drugs on clinical trials. It is anticipated that the development of simple, rapid, accurate, and low-cost genetic testing will promote research on pharmacogenetics and lead to the development of new drugs and therapy.

Acknowledgements

The work in my laboratory is supported by a Grant-in-Aid for Research on Sensory and Communicative Disorders from the Ministry of Health, Labor and Welfare of Japan; a Grant-in-Aid for Research on Advanced Medical Technology from the Ministry of Health, Labor and Welfare of Japan; a Grant-in Aid for Young Scientists (B) from the Japan Society for the Promotion of Science; the Takeda Science Foundation; the Mochida Memorial Foundation for Medical and Pharmaceutical Research; the Japan Research Foundation for Clinical Pharmacology; the Research Foundation for Pharmaceutical Sciences; and Suzuken Memorial Foundation.

References

[1] Evans WE, Relling MV. Pharmacogenomics: translating functional genomics into rational therapeutics. Science 1999;286:487–91.

[2] Goldstein DB, Tate SK, Sisodiya SM. Pharmacogenetics goes genomic. Nat Rev Genet 2003;4:937–47.

[3] Bert RJ, Granneman GR. Use of in vitro and in vivo data to estimate the likelihood of metabolic pharmacokinetic interactions. Clin Pharmacokinet 1997;32:210–58.

[4] Ingelman-Sundberg M, Oscarson M, McLellan RA. Polymorphic human cytochrome P450 enzymes: an opportunity for individualized drug treatment. Trends Pharmacol Sci 1999;20:342–9.

[5] Chida M, Yokoi T, Nemoto N, Inaba M, Kinoshita M, Kamataki T. A new variant CYP2D6 allele (CYP2D6*21) with a single base insertion in exon 5 in a Japanese population associated with a poor metabolizer phenotype. Pharmacogenetics 1999;9:287–93.

[6] Nishida Y, Fukuda T, Yamamoto I, Azuma J. CYP2D6 genotypes in a Japanese population: low frequencies of CYP2D6 gene duplication but high frequency of CYP2D6*10. Pharmacogenetics 2000;10: 567–570.

[7] Koyama E, Sohn DR, Shin SG, et al. Metabolic disposition of imipramine in Oriental subjects: relation to metoprolol alpha-hydroxylation and *S*-mephenytoin 4′-hydroxylation phenotypes. J Pharmacol Exp Ther 1994;271:860–7.

[8] Daly AK, Brockmoller J, Broly F, et al. Nomenclature for human CYP2D6 alleles. Pharmacogenetics 1996;6:193–201.

[9] Johansson I, Oscarson M, Yue QY, Bertilsson L, Sjoqvist F, Ingelman-Sundberg M. Genetic analysis of the Chinese cytochrome P4502D locus: characterization of variant CYP2D6 genes present in subjects with diminished capacity for debrisoquine hydroxylation. Mol Pharmacol 1994;46:452–9.

[10] Takahashi H, Kashima T, Nomoto S, et al. Comparisons between in-vitro and in-vivo metabolism of (*S*)-warfarin: catalytic activities of cDNA-expressed CYP2C9, its Leu359 variant and their mixture versus unbound clearance in patients with the corresponding CYP2C9 genotypes. Pharmacogenetics 1998;8:365–73.

[11] Takanashi K, Tainaka H, Kobayashi K, Yasumori T, Hosakawa M, Chiba K. CYP2C9 Ile359 and Leu359 variants: enzyme kinetic study with seven substrates. Pharmacogenetics 2000;10:95–104.

[12] Kidd RS, Straughn AB, Meyer MC, Blaisdell J, Goldstein JA, Dalton JT. Pharmacokinetics of chlorpheniramine, phenytoin, glipizide and nifedipine in an individual homozygous for the CYP2C9*3 allele. Pharmacogenetics 1999;9:71–80.

[13] Takahashi H, Kashima T, Nomizo Y, et al. Metabolism of warfarin enantiomers in Japanese patients with heart disease having different CYP2C9 and CYP2C19 genotypes. Clin Pharmacol Ther 1998; 63:519–28.

[14] Kimura M, Ieiri I, Mamiya K, Urae A, Higuchi S. Genetic polymorphism of cytochrome P450s, CYP2C19, and CYP2C9 in a Japanese population. Ther Drug Monit 1998;20:243–7.

[15] Ieiri I, Kubota T, Urae A, et al. Pharmacokinetics of omeprazole (a substrate of CYP2C19) and comparison with two mutant alleles, C gamma P2C19m1 in exon 5 and C gamma P2C19m2 in exon 4, in Japanese subjects. Clin Pharmacol Ther 1996;59:647–53.

[16] Furuta T, Ohashi K, Kosuge K, et al. CYP2C19 genotype status and effect of omeprazole on intragastric pH in humans. Clin Pharmacol Ther 1999;65:552–61.

[17] McLeod HL, Collie-Duguid ES, Vreken P, et al. Nomenclature for human DPYD alleles. Pharmacogenetics 1998;8:455–9.

[18] Collie-Duguid ES, Etienne MC, Milano G, McLeod HL. Known variant DPYD alleles do not explain DPD deficiency in cancer patients. Pharmacogenetics 2000;10:217–23.

[19] Wei X, McLeod HL, McMurrough J, Gonzalez FJ, Fernandez-Salguero P. Molecular basis of the human dihydropyrimidine dehydrogenase deficiency and 5-fluorouracil toxicity. J Clin Invest 1996;98:610–5.

[20] Etienne MC, Lagrange JL, Dassonville O, et al. Population study of dihydropyrimidine dehydrogenase in cancer patients. J Clin Oncol 1994;12:2248–53.

[21] Relling MV, Hancock ML, Rivera GK, et al. Mercaptopurine therapy intolerance and heterozygosity at the thiopurine S-methyltransferase gene locus. J Natl Cancer Inst 1999;91:2001–8.

[22] Evans DA. *N*-acetyltransferase. Pharmacol Ther 1989;42:157–234.

[23] Okumura K, Kita T, Chikazawa S, Komada F, Iwakawa S, Tanigawara Y. Genotyping of *N*-acetylation polymorphism and correlation with procainamide metabolism. Clin Pharmacol Ther 1997;61:509–17.

[24] Ohno M, Yamaguchi I, Yamamoto I, et al. Slow N-acetyltransferase 2 genotype affects the incidence of isoniazid and rifampicin-induced hepatotoxicity. Int J Tuberc Lung Dis 2000;4:256–61.

[25] Huang YS, Chern HD, Su WJ, et al. Polymorphism of the N-acetyltransferase 2 gene as a susceptibility risk factor for antituberculosis drug-induced hepatitis. Hepatology 2002;35:839–83.

[26] Ando Y, Saka H, Ando M, et al. Polymorphisms of UDP-glucuronosyltransferase gene and irinotecan toxicity: a pharmacogenetic analysis. Cancer Res 2000;60:6921–6.

[27] Wiebel FA, Dommermuth A, Thier R. The hereditary transmission of the glutathione transferase hGSTT1-1 conjugator phenotype in a large family. Pharmacogenetics 1999;9:251–66.

[28] Villafranca E, Okruzhnov Y, Dominguez MA, et al. Polymorphisms of the repeated sequences in the enhancer region of the thymidylate synthase gene promoter may predict downstaging after preoperative chemoradiation in rectal cancer. J Clin Oncol 2001; 19:1779–86.

[29] Paez JG, Janne PA, Lee JC, et al. EGFR mutations in lung cancer: correlation with clinical response to gefitinib therapy. Science 2004;304:1497–500.

[30] Lynch TJ, Bell DW, Sordella R, et al. Activating mutations in the epidermal growth factor receptor underlying responsiveness of non-small-cell lung cancer to gefitinib. N Engl J Med 2004;350: 2129–2139.

[31] Pao W, Miller V, Zakowski M, et al. EGF receptor gene mutations are common in lung cancers from "never smokers" and are associated with sensitivity of tumors to gefitinib and erlotinib. Proc Natl Acad Sci U S A 2004;101:13306–11.

[32] Shi MM, Bleavins MR, de la iglesia FA. Technologies for detecting genetic polymorphisms in pharmacogenomics. Mol Diagn 1999;4:343–51.

[33] Livak KJ, Flood SJ, Marmaro J, Giusti W, Deetz K. Oligonucleotides with fluorescent dyes at opposite ends provide a quenched probe system useful for detecting PCR product and nucleic acid hybridization. PCR Methods Appl 1995;4:357–62.

[34] Lay MJ, Wittwer CT. Real-time fluorescence genotyping of factor V Leiden during rapid-cycle PCR. Clin Chem 1997;43:2262–7.

[35] Lucas T, Losert D, Allen M, et al. Combination allele-specific real-time PCR for differentiation of beta 2-adrenergic receptor coding single-nucleotide polymorphisms. Clin Chem 2004;50:769–72.

[36] Teupser D, Rupprecht W, Lohse P, Thiery J. Fluorescence-based detection of the CETP TaqIB polymorphism: false positives with the TaqMan-based exonuclease assay attributable to a previously unknown gene variant. Clin Chem 2001;47:852–7.

[37] Hiratsuka M, Takekuma Y, Endo N, et al. Allele and genotype frequencies of CYP2B6 and CYP3A5 in the Japanese population. Eur J Clin Pharmacol 2002;58:417–21.

[38] Hiratsuka M, Agatsuma Y, Omori F, et al. High throughput detection of drug-metabolizing enzyme polymorphisms by allele-specific fluorogenic 5′ nuclease chain reaction assay. Biol Pharm Bull 2000;23:1131–5.

[39] Schaeffeler E, Schwab M, Eichelbaum M, Zanger UM. CYP2D6 genotyping strategy based on gene copy number determination by TaqMan real-time PCR. Hum Mutat 2003;22:476–85.

[40] Wong M, Balleine RL, Collins M, Liddle C, Clarke CL, Gurney H. CYP3A5 genotype and midazolam clearance in Australian patients receiving chemotherapy. Clin Pharmacol Ther 2004;75:529–38.

[41] Gross RL, Pratter MR, Schmidt MA, Bender PK. Leukotriene C4 synthase polymorphism analysis with the 5′ fluorogenic exonuclease (TaqMan) assay. Anal Biochem 2004;326:120–1.
[42] Saito K, Miyake S, Moriya H, et al. Detection of the four sequence variations of MDR1 gene using TaqMan MGB probe based real-time PCR and haplotype analysis in healthy Japanese subjects. Clin Biochem 2003;36:511–8.
[43] Hiratsuka M, Narahara K, Kishikawa Y, et al. A simultaneous LightCycler detection assay for five genetic polymorphisms influencing drug sensitivity. Clin Biochem 2002;35:35–40.
[44] Harth V, Bruning T, Abel J, et al. Real-time genotyping of cytochrome P4501A1 A4889G and T6235C polymorphisms. Mol Cell Probes 2001;15:93–7.
[45] Bruning T, Abel J, Koch B, et al. Real-time PCR-analysis of the cytochrome P450 1B1 codon 432-polymorphism. Arch Toxicol 1999;73:427–30.
[46] Muller B, Zopf K, Bachofer J, Steimer W. Optimized strategy for rapid cytochrome P450 2D6 genotyping by real-time long PCR. Clin Chem 2003;9:1624–31.
[47] Ko Y, Koch B, Harth V, et al. Rapid analysis of GSTM1, GSTT1 and GSTP1 polymorphisms using real-time polymerase chain reaction. Pharmacogenetics 2000;10:271–4.
[48] von Ahsen N, Richter M, Grupp C, Ringe B, Oellerich M, Armstrong VW. No influence of the MDR-1 C3435T polymorphism or a CYP3A4 promoter polymorphism (CYP3A4-V allele) on dose-adjusted cyclosporin A trough concentrations or rejection incidence in stable renal transplant recipients. Clin Chem 2001;47:1048–52.
[49] von Ahsen N, Schutz E, Armstrong VW, Oellerich M. Rapid detection of prothrombotic mutations of prothrombin (G20210A), factor V (G1691A), and methylenetetrahydrofolate reductase (C677T) by real-time fluorescence PCR with the LightCycler. Clin Chem 1999;45: 694–696.
[50] von Ahsen N, Oellerich M, Schutz E. A method for homogeneous color-compensated genotyping of factor V (G1691A) and methylenetetrahydrofolate reductase (C677T) mutations using real-time multiplex fluorescence PCR. Clin Biochem 2000;33:535–9.
[51] Brans R, Laizane D, Khan A, Blomeke B. *N*-acetyltransferase 2 genotyping: an accurate and feasible approach for simultaneous detection of the most common NAT2 alleles. Clin Chem 2004;50:1264–6.
[52] Blomeke B, Sieben S, Spotter D, Landt O, Merk HF. Identification of *N*-acetyltransferase 2 genotypes by continuous monitoring of fluorogenic hybridization probes. Anal Biochem 1999;275: 93–97.
[53] Schutz E, von Ahsen N, Oellerich M. Genotyping of eight thiopurine methyltransferase mutations: three-color multiplexing, "two-color/-shared" anchor, and fluorescence-quenching hybridization probe assays based on thermodynamic nearest-neighbor probe design. Clin Chem 2000;46:1728–37.
[54] Hiratsuka M, Agatsuma Y, Mizugaki M. Rapid detection of CYP2C9*3 alleles by real-time fluorescence PCR based on SYBR Green. Mol Genet Metab 1999;68:357–62.
[55] French DJ, Archard CL, Brown T, McDowell DG. HyBeacon probes: a new tool for DNA sequence detection and allele discrimination. Mol Cell Probes 2001;15:363–74.
[56] Latorra D, Campbell K, Wolter A, Hurley JM. Enhanced allele-specific PCR discrimination in SNP genotyping using 3′ locked nucleic acid (LNA) primers. Hum Mutat 2003;22:79–85.
[57] Liew M, Pryor R, Palais R, et al. Genotyping of single-nucleotide polymorphisms by high-resolution melting of small amplicons. Clin Chem 2004;50:1156–64.
[58] Zhou L, Myers AN, Vandersteen JG, Wang L, Wittwer CT. Closed-tube genotyping with unlabeled oligonucleotide probes and a saturating DNA dye. Clin Chem 2004;50:1328–35.
[59] Notomi T, Okayama H, Masubuchi H, et al. Loop-mediated isothermal amplification of DNA. Nucleic Acids Res 2000;28:E63.
[60] Frueh FW, Noyer-Weidner M. The use of denaturing high-performance liquid chromatography (DHPLC) for the analysis of genetic variations: impact for diagnostics and pharmacogenetics. Clin Chem Lab Med 2003;41:452–61.
[61] Zackrisson AL, Lindblom B. Identification of CYP2D6 alleles by single nucleotide polymorphism analysis using pyrosequencing. Eur J Clin Pharmacol 2003;59:521–6.
[62] Kwiatkowski RW, Lyamichev V, de Arruda M, Neri B. Clinical, genetic, and pharmacogenetic applications of the Invader assay. Mol Diagn 1999;4:353–64.
[63] Nevilie M, Selzer R, Aizenstein B, et al. Characterization of cytochrome P450 2D6 alleles using the Invader system. BioTechniques 2002:40–3 [Suppl].
[64] Pickering JW, McMillin GA, Gedge F, Hill HR, Lyon E. Flow cytometric assay for genotyping cytochrome p450 2C9 and 2C19: comparison with a microelectronic DNA array. Am J Pharmacogenomics 2004;4:199–207.
[65] Tang K, Fu DJ, Julien D, Braun A, Cantor CR, Koster H. Chip-based genotyping by mass spectrometry. Proc Natl Acad Sci U S A 1999;96:10016–20.
[66] Bell PA, Chaturvedi S, Gelfand CA, et al. SNPstream UHT: ultra-high throughput SNP genotyping for pharmacogenomics and drug discovery. BioTechniques 2002; Suppl:70-2, 74, 76-77.
[67] Huang JX, Mehrens D, Wiese R, et al. High-throughput genomic and proteomic analysis using microarray technology. Clin Chem 2001;47:1912–6.
[68] Borsting C, Sanchez JJ, Morling N. SNP typing on the NanoChip electronic microarray. Methods Mol Biol 2004;297:155–68.
[69] Matsubara Y, Kure S. Detection of single nucleotide substitution by competitive allele-specific short oligonucleotide hybridization (CASSOH) with immunochromatographic strip. Hum Mutat 2003; 22:166–72.
[70] Hiratsuka M, Ebisawa A, Matsubara Y, et al. Genotyping of single nucleotide polymorphisms (SNPs) influencing drug response by competitive allele-specific short oligonucleotide hybridization (CASSOH) with immunochromatographic strip. Drug Metab Pharmacokineti 2004;19:303–7.
[71] Hiratsuka M, Kishikawa Y, Takekuma Y, et al. Genotyping of the *N*-acetyltransferase2 Polymorphism in the Prediction of Adverse Drug Reactions to Isoniazid in Japanese Patients. Drug Metab Pharmacokineti 2002;17:357–62.
[72] Furuta T, Ohashi K, Kamata T, et al. Effect of genetic differences in omeprazole metabolism on cure rates for *Helicobacter pylori* infection and peptic ulcer. Ann Intern Med 1998;129:1027–30.
[73] Furuta T, Shirai N, Takashima M, et al. Effect of genotypic differences in CYP2C19 on cure rates for *Helicobacter pylori* infection by triple therapy with a proton pump inhibitor, amoxicillin, and clarithromycin. Clin Pharmacol Ther 2001;69:158–68.
[74] McLeod HL, Lin JS, Scott EP, Pui CH, Evans WE. Thiopurine methyltransferase activity in American white subjects and black subjects. Clin Pharmacol Ther 1994;55:15–20.
[75] Krynetski EY, Evans WE. Pharmacogenetics of cancer therapy: getting personal. Am J Hum Genet 1998;63:11–6.
[76] Prezant TR, Agapian JV, Bohlman MC, et al. Mitochondrial ribosomal RNA mutation associated with both antibiotic-induced and non-syndromic deafness. Nat Genet 1993;4:289–94.
[77] Cortopassi G, Hutchin T. A molecular and cellular hypothesis for aminoglycoside-induced deafness. Hear Res 1994;78:27–30.
[78] Usami S, Abe S, Shinkawa H, Inoue Y, Yamaguchi T. Rapid mass screening method and counseling for the 1555A→G mitochondrial mutation. J Hum Genet 1999;44:304–7.
[79] Tavadia SM, Mydlarski PR, Reis MD, et al. Screening for azathioprine toxicity: a pharmacoeconomic analysis based on a target case. J Am Acad Dermatol 2000;42:628–32.
[80] Desta Z, Zhao X, Shin JG, Flockhart DA. Clinical significance of the cytochrome P450 2C19 genetic polymorphism. Clin Pharmacokinet 2002;41:913–58.

© 2005 Wiley-Liss, Inc.

Rapid Publication

HRAS Mutation Analysis in Costello Syndrome: Genotype and Phenotype Correlation

Karen W. Gripp,[1]* Angela E. Lin,[2] Deborah L. Stabley,[3] Linda Nicholson,[1] Charles I. Scott Jr.,[1] Daniel Doyle,[4] Yoko Aoki,[5] Yoichi Matsubara,[5] Elaine H. Zackai,[6] Pablo Lapunzina,[7] Antonio Gonzalez-Meneses,[8] Jennifer Holbrook,[3] Cynthia A. Agresta,[3] Iris L. Gonzalez,[3] and Katia Sol-Church[3]

[1]Division of Medical Genetics, A. I. duPont Hospital for Children, Wilmington, Delaware
[2]Genetics and Teratology Unit, MassGeneral Hospital for Children, Boston, Massachusetts
[3]Department of Biomedical Research, Nemours' Childrens Clinic, Wilmington, Delaware
[4]Division of Endocrinology, A. I. duPont Hospital for Children, Wilmington, Delaware
[5]Department of Medical Genetics, Tohoku University School of Medicine, Sendai, Japan
[6]Department of Human Genetics, The Children's Hospital of Philadelphia, Philadelphia, Pennsylvania
[7]Department of Genetics, Hospital Universitario La Paz, Madrid, Spain
[8]Service de Dysmorphology, Hospital Universitario Virgen del Rocio, Sevilla, Spain

Received 5 October 2005; Accepted 20 October 2005

Costello syndrome is a rare condition comprising mental retardation, distinctive facial appearance, cardiovascular abnormalities (typically pulmonic stenosis, hypertrophic cardiomyopathy, and/or atrial tachycardia), tumor predisposition, and skin and musculoskeletal abnormalities. Recently mutations in *HRAS* were identified in 12 Japanese and Italian patients with clinical information available on 7 of the Japanese patients. To expand the molecular delineation of Costello syndrome, we performed mutation analysis in 34 North American and 6 European (total 40) patients with Costello syndrome, and detected missense mutations in *HRAS* in 33 (82.5%) patients. All mutations affected either codon 12 or 13 of the protein product, with G12S occurring in 30 (90.9%) patients of the mutation-positive cases. In two patients, we found a mutation resulting in an alanine substitution in position 12 (G12A), and in one patient, we detected a novel mutation (G13C). Five different *HRAS* mutations have now been reported in Costello syndrome, however genotype–phenotype correlation remains incomplete. © 2005 Wiley-Liss, Inc.

Key words: bladder cancer; gain-of-function; *HRAS*; overgrowth syndrome; rhabdomyosarcoma

INTRODUCTION

Costello syndrome (OMIM #218040) is a rare disorder with a distinctive prenatal phenotype (polyhydramnios, overgrowth, edema), postnatal feeding difficulties and failure to thrive, characteristic facial appearance, abnormalities of the heart, skin and musculoskeletal system, and tumor predisposition [reviewed by Hennekam, 2003; Gripp, 2005; Lin et al., 2005]. The risk of neoplasia (approximately 10–15%) [Gripp et al., 2002] influences clinical care, morbidity, and mortality. While the papillomata, which develop throughout childhood in the peri-oral and/or peri-anal region are the most common benign tumors, the most common malignancy is rhabdomyosarcoma (RMS), typically with embryonal histologic findings [reviewed by Gripp, 2005]. Less common are neuroblastoma, ganglioneuroblastoma, and transitional cell carcinoma of the bladder [Gripp, 2005].

Costello syndrome shares many phenotypic traits with cardio-facio-cutaneous (CFC) syndrome (OMIM #115150), and in some children it may be difficult if not impossible to be certain about the diagnosis. Although Costello, CFC, and Noonan syndrome (OMIM #163950) all share the familiar cardiac phenotype of pulmonic stenosis and/or hypertrophic cardiomyopathy [summarized in Table VII, Lin et al., 2002], the facial appearance and overall phenotype of Noonan syndrome is much less similar

Grant sponsor: Nemours Biomedical Research; Grant sponsor: NIH; Grant number: 1 P20 RR020173-01.
*Correspondence to: Karen W. Gripp, Division of Medical Genetics, A. I. duPont Hospital for Children, PO Box 269, Wilmington, DE 19899. E-mail: kgripp@nemours.org
DOI 10.1002/ajmg.a.31047

WILEY InterScience® DISCOVER SOMETHING GREAT

to Costello syndrome except in the fetal and neonatal period. Noonan syndrome is caused by missense mutations in *PTPN11*, encoding the tyrosine phosphatase SHP2, in about 50% of patients [Tartaglia et al., 2001]. These *PTPN11* mutations lead to a gain-of-function of SHP2 with enhanced phosphatase activity, resulting in increased activation of the mitogen activated protein kinase (MAPK) pathway. Aoki et al. [2005] hypothesized that the gene mutated in Costello syndrome encodes a molecule that functions upstream or downstream of SHP2 in the signal pathway. They identified the *RAS* genes as potential candidates and subsequently showed that germline mutations in *HRAS* are the underlying cause of Costello syndrome. The mutations identified by Aoki et al. [2005] affect one of two amino acids (position 12 and 13 of the protein) previously found to be mutated in malignant tumors.

To increase our understanding of the molecular definition of Costello syndrome and to provide clinical correlation, we report the results of mutation analysis and phenotypic review in 40 North American and European patients.

MATERIAL AND METHODS

Patients

Patients with Costello syndrome were identified at the 2003 and 2005 International Costello Syndrome Meetings, through the Costello Syndrome Family Network and through physician referral. Patients 1–27 and 29–36 (Table I) were enrolled in a research study approved by the Institutional Review Board of the A. I. duPont Hospital for Children (#2003–006). Clinical information was obtained by self-report by the families who completed a standardized data collection form which was updated every 2 years, when possible, and supplemented by review of medical records and interview of the families. Additional patients (Table I, Patients 28, 37–40) were clinically identified by P.L. and A. G.-M. and studied under an IRB approved protocol (CEIC-HULP-2003-PI-362) at the Hospital Universitario La Paz, Madrid, Spain.

Although a patient may have been diagnosed by a local geneticist or other professional, the diagnosis of Costello syndrome was confirmed independently by K.W.G. and A.E. L. based on diagnostic guidelines [Table 14.1, Lin et al., 2005; Proud et al., 2005]. Emphasis was placed on the characteristic growth pattern (especially severe feeding problems and failure to thrive), developmental delay or mental retardation, skin abnormalities, and distinctive hands, especially ulnar deviation, and ligamentous laxity of the fingers. The characteristic craniofacial appearance (macrocephaly, high forehead, unusually curly hair, hypertelorism, fleshy nasal tip, full lips, wide mouth, full cheeks, and fleshy ear lobes) was the most discriminatory and created the most discussion and doubt in diagnosis when atypical. In this series of well-scrutinized patients, all patients had many of these facial findings. Cardiac hypertrophy included hypertrophic cardiomyopathy (also known as asymmetric septal hypertrophy and idiopathic hypertrophic subaortic stenosis), but excluded mild septal thickening [Lin et al., 2002]. Cardiovascular malformations referred to structural congenital heart defects, and excluded valve prolapse, regurgitation, dysplasia, or thickening.

Laboratory Techniques

DNA was extracted from blood, saliva, or cell lines using standard methods. All DNA represents constitutional samples, no tumor samples were analyzed. In the patients enrolled in the North American protocol, genomic DNA was extracted from buccal cells, blood, or from previously established fibroblast cultures using the PureGene DNA Isolation Kit (Gentra Systems, Minneapolis, MN). Genomic DNA was isolated from saliva samples using the Oragen purification kit. A discrete 575 bp region of the *HRAS* gene containing the first translated exon (Exon 2) and flanking intronic regions was amplified by polymerase chain reaction using these primers: forward-ATTTGGGTGCGTGGTTGA, reverse-CCTCTAGAG-GAAGCAGGAGACA. PCR was performed with 150 ng genomic DNA in a 25 μl reaction containing 1× Qiagen Taq Buffer plus Q solution, 3 mM $MgCl_2$, 500 μM each dNTP, 1 μM of each forward and reverse primers and 0.75 U Taq polymerase (Qiagen, Valencia, CA). Reactions were run on a Stratagene robocycler for 30 cycles (30 sec at 94°C, 30 sec at 60°C, and 1 min at 72°C). Genomic fragments containing the remaining translated exons were amplified in the presence of Q-solution and an annealing temperature of 63°C, using primers previously described [Aoki et al., 2005]. Sequencing was performed in both directions using the ABI BigDye Terminator Cycle Sequencing Ready Reaction kit v 3.1, using a 1/4 dilution of the terminator mix, and analyzed on an ABI3130XL Genetic Analyzer.

The protocol used for the Spanish patients varied regarding the primer sequences and reaction conditions used. Polymerase chain reaction and sequencing were performed following standard protocols [Cheng et al., 1994; Williams and Soper, 1995].

We sequenced the entire coding region in all patients in whom no disease causing mutation was identified. Parental samples were sequenced as available, for the amplicon of interest only.

RESULTS

Table I presents the clinical and molecular characteristics of 40 patients (34 North American,

TABLE I. Genotype and Phenotype Analysis in 40 Patients With Costello Syndrome

	Mutation				Growth			Clinical features								Cardiac abnormalities		
Pt#	Nucleotide substitution	Amino acid change	Sex	Age	Ht centile	OFC centile	GH deficiency	Polyhydramnios	FTT	Tone	CNS abnormality	Nystagmus	Ulnar deviation	Papillomata	Tumor	Cardiac hypertrophy	Arrhythmia	CVM
1[a]	34G→A	G12S	F	4	−5 SD	90th	–	+	+	↑	–	+	+	–	–	–	SVT	PS
2	34G→A	G12S	F	10	−5 SD	50–75th	–	+	+	↓	Chiari I syrinx	+	+	–	–	–	–	–
3[b,c]	34G→A	G12S	M	22	−5 SD	90th	–	+	+	↓	–	–	+	+	–	HCM severe concentric	SVT, PACs, PVCs	BAV
4[c]	34G→A	G12S	F	28	−4 SD	>98th	+	+	+	–	–	+	–	+	–	–	–	–
5[b]	34G→A	G12S	F	8	−5 SD	3–10th	–	+	+	↓	–	–	+	+	–	HCM	SVT	ASD
6	34G→A	G12S	M	4	−3 SD	90–97th	–	+	+	↓	–	+	–	–	–	–	SVT	–
7[c]	34G→A	G12S	F	20	10th	75th	+Rec'd GH	+	+	↓	–	–	+	+	–	–	+	–
8[a]	34G→A	G12S	F	2	−4SD	75–90th	–	+	+	↓	–	+	+	–	–	HCM	Tachycardia NOS	–
9	34G→A	G12S	M	5	−4 SD	50–75th	+Rec'd GH	+	+	↓	–	–	+	–	–	–	–	–
10[a,e]	34G→A	G12S	F	6	−4 SD	>98th	+Rec'd GH	+	+	↓	–	+	+	+	–	LVH concentric	–	PSV, VSD
11[b,f,g]	34G→A	G12S	F	9	−5 SD	>98th	+Rec'd GH	+	+	–	VM	+	+	+	RMS	HCM Severe	SVT, EAT	PSV, MS
12[c]	34G→A	G12S	M	35	−4 SD	>98th	–	–	+	↓	–	–	+	+	–	–	–	PSV, ASD
13	34G→A	G12S	F	3	−5 SD	75th	+	+	+	↓	Chiari I	–	–	–	–	HCM	Severe sinus tachycardia	–
14	34G→A	G12S	M	7	−5 SD	50–75th	+	+	+	–	+	–	–	–	–	–	–	
15[b]	34G→A	G12S	F	9	−5 SD	50th	–	+	+	↓	HC, VPS, Chiari I	+	+	+	–	–	Tachycardia, Bradycardia	PSV
16	34G→A	G12S	F	17	−3 SD	>98th	+ Rec'd GH	+	+	↓	–	+	+	+	Benign bladder tumor	–	–	–
17	34G→A	G12S	F	10	1–3rd	90th	+ Rec'd GH	–	+	↓	–	–	+	+	–	–	–	–
18[d]	34G→A	G12S	M	16	−5 SD	90th	+ Rec'd GH	+	+	↓	VM	+	+	–	–	LVH	–	–
19[a,b]	34G→A	G12S	F	10	1–3rd	50–75th	–	+	+	↓	–	–	–	–	–	–	–	–
20	34G→A	G12S	M	3	−5 SD	50–75th	–	+	+	↓	–	–	+	+	–	HCM	SVT	–
21	34G→A	G12S	F	6	−5 SD	50–75th	–	+	+	–	–	–	–	–	–	–	–	–
22	34G→A	G12S	F	13	−4 SD	75–90th	+ Rec'd GH	+	+	–	–	–	+	+	–	–	LQTS	–
23	34G→A	G12S	M	19	−4 SD	>98th	–	+	+	↓	–	–	+	+	–	HCM	–	–
24	34G→A	G12S	F	6	−5 SD	>98th	–	+	+	–	–	+	+	–	–	HCM Severe	+ NOS	–
25	34G→A	G12S	M	10	−4 SD	75th	+	+	+	↓	–	–	+	–	–	–	–	–
26[b,h]	34G→A	G12S	M	10	−5 SD	25th	+ Rec'd GH	+	+	–	Chiari I	–	+	–	–	–	–	PSV
27	34G→A	G12S	F	9	−3 SD	>98th	–	+	+	–	HC, VPS	+	–	–		–	–	–
28[k]	34G→A	G12S	M	8	−4 SD	25–50th	–	+	+	↓	HC	+	+	–	–	IHSS	SVT	PS, ASD
29	34G→A	G12S	M	2	−4 SD	50th	+	+	+	–	–	–	+	–	RMS	+	EAT	–
30[c,h,i]	34G→A	G12S	F	16	5th	>98th	+ Rec'd GH	–	+	↓	–	–	+	+	–	+	–	–
31[a]	35G→C	G12A	M	6	−4 SD	75th	–	+	+	↓	HC, VPS	+	+	+	–	–	Sinus tachycardia, persistent	–
32[c,j]	35G→C	G12A	F	21	−5 SD	75–90th	+ Rec'd GH	–	+	–	–	–	–	+	Bladder CA	–	–	–
33[b]	37G→T	G13C	M	12	5th	>98th	–	+	+	↓	VM	–	–	–	–	LVH	–	–
Patients with No *HRAS* Mutation:																		
34*[a]	None		M	6	−3 SD	50–75th	–	–	+	↓	–	–	+	–	–	–	–	–
35[a]	None		F	2	−5 SD	10–25th	–	+	+	↓	Increased extra axial fluid	+	+	–	–	HCM	–	PSV
36*	None		M	6	−5 SD	>98th	–	+	+	↓	HC	+	+	–	–	HCM	EAT, PVC, PAC	–
37*[k]	None		F	1	−3 SD	10th	–	–	+	↓	–	–	–	–	–	–	–	SVPS
38*[k]	None		M	3	−3 SD	10–25th	–	+	+	↓	VM	+	+	–	–	–	–	–
39*[k]	None		M	4	−3 SD	NA	–	–	+	↓	Hypoplastic CC, Mega cisterna magna	–	–	–	–	–	–	PS
40*[k]	None		F	4	−4 SD	50–75th	–	+	–	↓	–	–	–	–	–	+ NOS	SVT	PS

ASD, atrial septal defect; BAV, bicuspid aortic valve; CA, carcinoma; CAR, chaotic atrial rhythm; CC, corpus callosum; CNS, central nervous system; CVM, cardiovascular malformation; EAT, ectopic atrial rhythm; F, female; FTT, failure to thrive; GH, growth hormone; HC, hydrocephalus; HCM, hypertrophic cardiomyopathy; Ht, height; IHSS, idiopathic subaortic stenosis; LQTS, prolongation of QT interval; M, male; MS, mitral stenosis; NA, not available; NOS, not otherwise specified; PSV/SV, pulmonic stenosis (valvar, supravalvar); PAC, premature atrial contraction; Pt, patient; RMS, rhabdomyosarcoma; SVT, supraventricular tachycardia; Tone increased (↑), tone decreased (↓); VM, ventriculomegaly; VPS, ventriculo-peritoneal shunt; VSD, ventricular septal defect. Age in years, at time measurements for height and OFC were obtained. Height as percentile, or standard deviation when below 1st centile.

Reported previously.

[a]Gripp et al. [2004].

[b]Lin et al. [2002].

[c]White et al. [2005].

[d]Johnson et al. [1998].

[e]Lin et al. [2004].

[f]Dearlove and Harper [1997].

[g]Kerr et al. [1998].

[h]Stein et al. [2004].

[i]Legault and Gagnon [2001].

[j]Gripp et al. [2000].

[k]Spanish patients.

*Indicates overall appearance which was not classic or atypical for Costello syndrome.

American Journal of Medical Genetics: DOI 10.1002/ajmg.a

6 European) with Costello syndrome. There were 22 females (55%). Ages ranged from 2 to 35 years.

We identified heterozygous *HRAS* mutations in 33 of 40 (82.5%) patients. All mutations occurred de novo, since none of the 19 sets of analyzed parents carried the sequence change. The *HRAS* mutations were identified in different cell types in two patients (Table I, Patient 14: buccal cells and lymphocytes; Patient 18: fibroblasts and lymphocytes) for which different tissues were available, thus indicating that these mutations occurred in the parental germline. Most (30 of 33, 90.9%) of the mutations are 34G > A nucleotide transitions resulting in the substitution of a serine for the glycine in position 12 (G12S). We identified two additional patients with a 35G > C transversion resulting in an alanine substitution in position 12 (G12A). A 37G > T mutation seen in one patient causing a cysteine substitution of amino acid 13 (G13C) has not previously been reported in Costello syndrome (Table II). Table I lists the presumed disease causing nucleotide changes. Several novel single nucleotide polymorphisms (SNPs) were identified in mutation-positive and -negative patients (data not shown). These SNPs were also present in parents and control DNAs isolated from unrelated volunteers and do not appear related to Costello syndrome.

Table III presents a comparison of the clinical characteristics between patients with and without mutations, and between the different mutations.

DISCUSSION

Our results confirm that germline *HRAS* mutations cause Costello syndrome in most patients [Aoki et al., 2005]. All mutations occurred de novo among those triads tested (slightly over half). The patients' missense mutations result in amino acid substitutions of a glycine residue in position 12 or 13 of the protein product. These particular amino acids are located at the GTP binding site and mutations at these sites have previously been shown to cause constitutive activation of HRAS, in turn causing increased activation of downstream effectors in signaling pathways controlling cell proliferation and differentiation [Oliva et al., 2004].

Based on a total of 45 (12 Aoki et al., 2005; 33 in this study) patients with mutations, mutations affecting HRAS amino acids 12 and 13 seem to define a mutational hotspot for Costello syndrome. The phosphate (PO_4) box of the HRAS GTP binding domain encoded by amino acid 10–15 in Exon 2 includes several 5′-CG-3′ (CpG) sites, which could account for this mutational hotspot. When these CpGs are methylated, they become vulnerable to mutations affecting not only the cytosines of either DNA strand, but also the neighboring guanines [Pfeifer, 2000]. Spontaneous mutations can occur at these sites, especially C → T or G → A transitions, with the G → A mutation resulting in the G12S change seen in 30 Costello patients reported here, and 7 previously reported (Table II).

In contrast, nearly 80% of codon 12 mutations seen in tumors [Sanger Institute Catalogue of Somatic Mutations in Cancer, 2005], involve a G → T transversion resulting in amino acid changes G12V or G12C (Table II). The frequency of these mutations is increased in response to mutagens acting on methylated CpG and are very common in many tumor tissues, indicating a high oncogenic potential resulting from the constitutive activation of the protein product. As pointed out by Aoki et al. [2005], the *HRAS* mutation spectrum seen in Costello syndrome differs both qualitatively and quantitatively from the mutation spectrum seen in tumors. The lack of mutations affecting codons other than those in malignancies suggests that there are a limited number of codons in which missense mutations can lead to constitutive activation of the protein product.

Heterozygous missense mutations causing constitutive activation of the protein product often occur in the paternal germline, as suggested by Penrose [1955] who proposed that mitotic replications errors accumulate in male germ cells. Supporting this hypothesis are the findings in Apert syndrome, achondroplasia and Muenke syndrome, due to missense mutations in *FGFR2* and *FGFR3*, respectively, with exclusive paternal origin of new mutations resulting in constitutive activation or increased ligand binding of the protein product [Moloney et al., 1996; Rannan-Eliya et al., 2004]. The paternal age effect observed in Costello syndrome [Lurie, 1994], in combination with

TABLE II. *HRAS* Mutations in Patients With Costello Syndrome and in Tumor Samples

Amino acid change	Nucleotide substitution	Aoki et al. [2005]	This report	Total (%)	Frequency in tumors[a]
G12S	34G → A	7	30	37 (82.2 %)	6.5%
G12A	35G → C	2	2	4 (8.8 %)	0.4%
G13D	38G → A	2	—	2 (4.4 %)	4.4%
G12V[b]	35GC → TT; 35G → T	1	—	1 (2.2%)	44.2%
G13C	37G → T	—	1	1 (2.2%)	0.6%

[a]Frequency in tumors was calculated based on 477 *HRAS* missense mutation positive tumor samples on the Sanger Institute Catalogue of Somatic Mutations in Cancer [2005]. Percentages in the tumors do not add up to 100 because only the amino acid changes seen in Costello syndrome are listed.
[b]The G12V mutations is typically due to a G to T transversion at position 35 in tumors; however, in the Costello patient, a double mutation occurred resulting in the same predicted amino acid change.

TABLE III. Clinical Characteristics and *HRAS* Mutation Status in Patients With Costello Syndrome: Combined Series

		HRAS mutation present					
Clinical characteristic	No mutation 7 (7,0) pts	Total 40[a] (33,7) pts	G12S 33 (30,3) pts	G12A 3 (2,1) pts	G13D 2 (0,2) pts	G12V 1 (0,1) pt	G13C 1 (1,0) pt
Failure to thrive	6/7 (86%)	40/40 (100%)	33/33 (100%)	G13D 2 (0,2) pts	G12V 1 (0,1) pt	G13C 1 (1,0) pt	1/1 (100%)
Polyhydramnios	4/7 (57%)	29/33 (87%)	27/30 (90%)	1/2 (50%)	N/A	N/A	1/1 (100%)
Hypotonia	7/7 (100%)	24/33 (72%)	22/30 (73%)	1/2 (50%)	N/A	N/A	1/1 (100%)
Ulnar deviation	4/7 (57%)	25/33 (75%)	24/30 (80%)	1/2 (50%)	N/A	N/A	0/1 (0%)
Any cardiac abnormality	5/7 (71%)	30/40 (75%)	22/33 (66%)	2/3 (66%)	2/2 (100%)	1/1 (100%)	1/1 (100%)
Cardiac hypertrophy	4/7 (43%)	19/40 (47%)	15/33 (45%)	1/3 (33%)	1/2 (50%)	1/1 (100%)	1/1 (100%)
Arrhythmia	2/7 (28%)	17/40 (42%)	15/33 (45%)	1/3 (33%)	1/2 (50%)	0/1 (0%)	0/1 (0%)
CVM	4/7 (57%)	10/40 (25%)	9/33 (27%)	0/3 (0%)	1/2 (50%)	0/1 (0%)	0/1 (0%)
Papillomata	0/7 (0%)	19/40 (47%)	16/33 (48%)	2/3 (66%)	1/2 (50%)	0/1 (0%)	0/1 (0%)
GH deficiency	0/7 (0%)	15/33 (45%)	14/30 (46%)	1/2 (50%)	N/A	N/A	0/1 (0%)
Nystagmus	3/7 (43%)	14/33 (42%)	13/30 (43%)	1/2 (50%)	N/A	N/A	0/1 (0%)
Tumor	0/7 (0%)	6/40 (15%)	4/33 (12%)	2/3 (66%)	0/2 (0%)	0/1 (0%)	0/1 (0%)
CNS abnormality	4/7 (57%)	9/33 (27%)	8/30 (27%)	1/2 (50%)	N/A	N/A	1/1 (100%)

Figures are rounded.

CNS, central nervous system abnormality; CVM, cardiovascular malformation; GH, growth hormone.

[a]Patient total includes the 33 new patients listed on Table I in this report, and the 7 Japanese patients listed on the supplementary Table I (online version) of Aoki et al. [2005]; no information was available on the five Italian patients from that series. Patients are listed as the total, followed in parentheses by the number in the present series and Japanese patients. There was no information on polyhydramnios, growth hormone deficiency, hypotonia, nystagmus, and ulnar deviation was provided by Aoki et al. [2005], and thus, denominators reflect the number of informative patients.

the nature of the missense mutations, suggests a paternal origin of the mutations. In this context, the loss of heterozygosity (LOH) of 11p15.5 in tumor tissue from Costello syndrome cases is of particular interest. Kerr et al. [2003] analyzed five embryonal RMS from Costello syndrome patients and showed loss of heterozygosity for 11p15.5 in all samples, with retention of the paternal allele confirmed in two cases. This finding may be consistent with the monoallelic expression of the mutated allele in the ganglioneuroblastoma described by Aoki et al. [2005]. It remains to be seen if LOH for *HRAS* is a consistent finding in all tumors in Costello syndrome, or if it is typical only for embryonal tumors as reported by Kerr et al. [2003] and Aoki et al. [2005]. While the constitutional *HRAS* mutation in Costello patients represents the first step in tumorigenesis, the second step may vary with LOH in embryonal tumors and mutations in additional genes in bladder cancer and other malignancies of adulthood. Jebar et al. [2005] reviewed *FGFR3* and *RAS* mutations in urothelial cell carcinoma and did not identify LOH, rather they reported mutually exclusive sequence changes in the genes whose protein products share the MAPK pathway as common effector.

The lack of mutations in seven patients led us to review their respective clinical presentation in detail. All patients except Patients 34 and 36 enrolled under the North American study were thought to have the typical facial changes of Costello syndrome. Upon review of facial photographs of the patients enrolled under the Spanish protocol, only Patient 28 had the completely characteristic facial appearance of Costello syndrome, and Patients 37–40 had facial findings consistent with either Costello or CFC syndrome. At this time, we cannot be certain that the lack of an identifiable *HRAS* mutation excludes the diagnosis of Costello syndrome. The possibility that these patients do not have Costello, but possibly CFC syndrome needs to be considered. If this was confirmed, the phenotype of CFC syndrome would include elevated catecholamine metabolite levels and cardiac arrhythmia.

It is noteworthy that we identified *HRAS* mutations in Patients 11, 29, and 30, who each had a malignancy, and Patient 16, who reportedly had a benign bladder tumor. Patient 30 developed a transitional cell carcinoma of the bladder [Gripp et al., 2000], she carries a mutation predicted to result in a G12A amino acid substitution. This mutation is found in less than 1% of malignancies with an *HRAS* mutation (Table II), specifically in one chondrosarcoma and one papillary thyroid carcinoma [Sanger Institute Catalogue of Somatic Mutations in Cancer, 2005]. In contrast, the G12S change present in Patients 11 and 29 with RMS represents the most common mutation in Costello syndrome and occurs in a variety of malignancies including soft tissue and synovial sarcoma and carcinoma of the gastro-intestinal and urinary tract [Sanger Institute Catalogue of Somatic Mutations in Cancer, 2005]. This mutation was seen in a Japanese patient with rhabdomyosarcoma [Aoki et al., 2005]. We identified one novel CS mutation, resulting in a cysteine substitution of amino acid 13 (Table I, Patient 33). This particular mutation is relatively rare in malignancies, but has been identified in three bladder cancer samples [Visvanathan et al., 1988; Levesque et al., 1993]. While it may be tempting to speculate on the oncogenic potential of the different mutations, we need more data to evaluate if the cancer risk varies by mutation.

Most of our patients and those reported by Aoki et al. [2005] share a common mutation (Table II). Rare phenotypic findings in these patients, for example

the long QT syndrome in Patient 22, may be coincidental, or caused by the mutation with a low incidence or in combination with modifying factors. A correlation between the cardiac abnormalities and the specific mutations is also hampered by the fact that we have few patients with mutations other than G12S. Of the three patients with mutations other than G12S, one each had left ventricular hypertrophy and tachycardia. While none had pulmonic stenosis or other structural anomalies, these numbers are too small to draw conclusions. Of note are the cardiac anomalies seen in some of the *HRAS* mutation-negative patients: Three had hypertrophic cardiomyopathy, two showed tachyarrhythmia, and four had pulmonic stenosis. Concerning the short stature seen in almost all Costello patients, Patient 33, the only person reported to date with the G13C mutation, is noteworthy. He is the tallest mutation-positive patient who never received growth hormone, and at age 12 years, he has not developed papillomata. This may suggest that G13C causes a slightly less severe phenotype.

The identification of *HRAS* mutations as the underlying cause for Costello syndrome is very helpful in respect to the ability to confirm a clinical diagnosis of Costello syndrome. Based on the data available today, a *HRAS* missense mutation leading to constitutive activation of the protein, in combination with consistent clinical findings, is likely diagnostic of Costello syndrome. In contrast, we cannot be certain that the lack of such a mutation precludes a diagnosis of Costello syndrome. It is too early to revise recommendations for clinical care based on the mutation status, but we hope to collect additional data in order to achieve this goal. Lastly, one may speculate that the identification of these mutations in Costello syndrome in combination with the knowledge from cancer research on *HRAS* and the MAPK pathway will allow for the use of medications directed at this pathway.

ACKNOWLEDGMENTS

We thank the families, individuals with Costello syndrome, and professionals of the Costello Syndrome support groups around the world, and Lisa Schoyer, president of the Costello Syndrome Family Network. This report was supported by Nemours Biomedical Research and by funds to KSC from NIH grant number 1 P20 RR020173-01 from the National Center for Research Resources.

REFERENCES

Aoki Y, Niihori T, Kawame H, Kurosawa K, Ohashi H, Tanaka Y, Filocamo M, Kato K, Suzuki Y, Kure S, Matsubara Y. 2005. Germline mutations in HRAS proto-oncogene cause Costello syndrome. Nat Genet 37:1038–1040.

Cheng S, Fockler C, Barnes WM, Higuchi R. 1994. Effective amplification of long targets from cloned inserts and human genomic DNA. Proc Natl Acad Sci USA 91:5695–5699.

Dearlove O, Harper N. 1997. Costello syndrome. Paediatr Anaesth 7:476–477.

Gripp KW. 2005. Tumor predisposition in Costello syndrome. Am J Med Genet 137C:72–77.

Gripp KW, Scott CI Jr, Nicholson L, Figueroa TE. 2000. A second case of bladder carcinoma in a patient with Costello syndrome. Am J Med Genet 90:256–259.

Gripp KW, Scott CI Jr, Nicholson L, McDonald-McGinn DM, Ozeran JD, Jones MC, Lin AE, Zackai EH. 2002. Five additional Costello syndrome patients with rhabdomyosarcoma: Proposal for a tumor screening protocol. Am J Med Genet 108: 80–87.

Gripp KW, Kawame H, Viskochil DH, Nicholson L. 2004. Elevated catecholamine metabolites in patients with Costello syndrome. Am J Med Genet 128A:48–51.

Hennekam RCM. 2003. Costello syndrome: An overview. Am J Med Genet 117C:42–48.

Jebar AH, Hurst CD, Tomlinson DC, Johnston C, Taylor CF, Knowles MA. 2005. FGFR3 and Ras gene mutations are mutually exclusive genetic events in urothelial cell carcinoma. Oncogene 24:5218–5225.

Johnson JP, Golabi M, Norton ME, Rosenblatt RM, Feldman GM, Yang SP, Hall BD, Fries MH, Carey JC. 1998. Costello syndrome: Phenotype, natural history, differential diagnosis, and possible cause. J Pediatr 133:441–448.

Kerr B, Eden TOB, Dandamudi R, Shannon N, Quarrell O, Emmerson A, Ladusans E, Gerrard M, Donnai D. 1998. Costello syndrome: Two cases with embryonal rhabdomyosarcoma. J Med Genet 335:1036–1039.

Kerr B, Mucchielli ML, Sigaudy S, Fabre M, Saunier P, Voelckel MA, Howard E, Elles R, Eden TOB, Black GC, Philip N. 2003. Is the locus for Costello syndrome on 11p?. J Med Genet 40:469–471.

Legault L, Gagnon C. 2001. Growth hormone deficiency in Costello syndrome: A possible explanation for the short stature. J Pediatr 138:151–152.

Levesque P, Ramchurren N, Saini K, Joyce A, Libertino J, Summerhayes IC. 1993. Screening of human bladder tumors and urine sediments for the presence of H-ras mutations. Int J Cancer 55:785–790.

Lin AE, Grossfeld PD, Hamilton R, Smoot L, Proud V, Weksberg R, Gripp KW, Wheeler P, Picker J, Irons M, Zackai EH, Scott CI, Nicholson L. 2002. Further delineation of cardiac anomalies in Costello syndrome. Am J Med Genet 111:115–129.

Lin AE, Harding C, Silberbach M. 2004. Hand it to the skin in Costello syndrome. J Pediatr 144:135.

Lin AE, Gripp KG, Kerr BK. 2005. Costello syndrome. In: Cassidy SB, Allanson JE, editors. Management of genetic syndromes. 2nd edition Hoboken: Wiley Liss, pp 151–162.

Lurie IW. 1994. Genetics of the Costello syndrome. Am J Med Genet 52:358–359.

Moloney DM, Slaney SF, Oldridge M, Wall SA, Sahlin P, Stenman G, Wilkie AO. 1996. Exclusive paternal origin of new mutations in Apert syndrome. Nat Genet 13:48–53.

Oliva JL, Zarich N, Martinez N, Jorge R, Castrillo A, Azanedo M, Garcia-Vargas S, Gutierrez-Eisman S, Juarranz A, Bosca L, Gutkind JS, Rojas JM. 2004. The P34G mutation reduces the transforming activity of K-Ras and N-Ras in NIH 3T3 cells but not of H-Ras. J Bio Chem 279:33480–33489.

Penrose LS. 1955. Parental age and mutation. Lancet 2:312–313.

Pfeifer GP. 2000. p53 mutational spectra and the role of methylated CpG sequences. Mutat Res 450:155–166.

Proud VK, Creswick HA, Schoyer L. 2005. Costello syndrome: Developing diagnostic criteria. Proc Greenwood Genet Ctr 24:126A.

Rannan-Eliya SV, Taylor IB, De Heer IM, Van Den Ouweland AM, Wall SA, Wilkie A. 2004. Paternal origin of FGFR3 mutations in Muenke-type craniosynostosis. Hum Genet 115:200–207.

Sanger Institute Catalogue of Somatic Mutations in Cancer. 2005. Distribution of somatic mutations in HRAS. www.sanger.ac.uk

Stein RI, Legault L, Daneman D, Weksberg R, Hamilton J. 2004. Growth hormone deficiency in Costello syndrome. Am J Med Genet Part A 129A:166–170.

Tartaglia M, Mehler EL, Goldberg R, Zampino G, Brunner HG, Kremer H, van der Burgt I, Crosby AH, Ion A, Jeffery S, Kalidas K, Patton MA, Kucherlapati RS, Gelb BD. 2001. Mutations in PTPN11, encoding the protein tyrosine phosphatase SHP-2, cause Noonan syndrome. Nat Genet 29:465–468.

Visvanathan KV, Pocock RD, Summerhayes IC. 1988. Preferential and novel activation of H-ras in human bladder carcinomas. Oncogene Res 3:77–86.

White SM, Graham JM, Kerr B, Gripp K, Weksberg R, Cytrynbaum C, Reeder JL, Stewart FJ, Edwards M, Wilson M, Bankier A. 2005. The adult phenotype in Costello syndrome. Am J Med Genet 136A:128–135.

Williams DC, Soper SA. 1995. Ultrasensitive near-IR fluorescence detection for capillary gel electrophoresis and DNA sequencing applications. Anal Chem 67:3427–3432.

nature genetics

© 2006 Nature Publishing Group http://www.nature.com/naturegenetics

Germline *KRAS* and *BRAF* mutations in cardio-facio-cutaneous syndrome

Tetsuya Niihori[1], Yoko Aoki[1], Yoko Narumi[1], Giovanni Neri[2], Hélène Cavé[3], Alain Verloes[3], Nobuhiko Okamoto[4], Raoul C M Hennekam[5], Gabriele Gillessen-Kaesbach[6], Dagmar Wieczorek[6], Maria Ines Kavamura[7], Kenji Kurosawa[8], Hirofumi Ohashi[9], Louise Wilson[10], Delphine Heron[11], Dominique Bonneau[12], Giuseppina Corona[13], Tadashi Kaname[14], Kenji Naritomi[14], Clarisse Baumann[3], Naomichi Matsumoto[15], Kumi Kato[1,16], Shigeo Kure[1] & Yoichi Matsubara[1,16]

Cardio-facio-cutaneous (CFC) syndrome is characterized by a distinctive facial appearance, heart defects and mental retardation. It phenotypically overlaps with Noonan and Costello syndrome, which are caused by mutations in *PTPN11* and *HRAS*, respectively. In 43 individuals with CFC, we identified two heterozygous *KRAS* mutations in three individuals and eight *BRAF* mutations in 16 individuals, suggesting that dysregulation of the RAS-RAF-ERK pathway is a common molecular basis for the three related disorders.

Cardio-facio-cutaneous (CFC) syndrome (OMIM 115150) was first described in 1986 (ref. 1). Affected individuals present with heart defects, including pulmonic stenosis, atrial septal defects and hypertrophic cardiomyopathy, and ectodermal abnormalities such as sparse, friable hair, hyperkeratotic skin lesions and a generalized ichthyosis-like condition. Typical facial characteristics include high forehead with bitemporal constriction, hypoplastic supraorbital ridges, downslanting palpebral fissures, a depressed nasal bridge and posteriorly angulated ears with prominent helices. The molecular basis of CFC syndrome has remained unknown. There are phenotypic similarities between this syndrome, Noonan syndrome (OMIM 163950) and Costello syndrome (OMIM 218040)[2,3]. Gain-of-function mutations in protein tyrosine phosphatase SHP-2 (*PTPN11*) have been identified in approximately 40% of individuals with clinically diagnosed Noonan syndrome[4]. No *PTPN11* mutations have been found in individuals with CFC syndrome[5–7]. Recently, we identified *HRAS* mutations in 12 of 13 individuals with Costello syndrome[8]. These findings suggest that the activation of the RAS-MAPK pathway is the common underlying mechanism of Noonan syndrome and Costello syndrome and, hence, possibly of CFC syndrome.

To elucidate the molecular basis of CFC syndrome, we first sequenced the entire coding regions of three RAS genes, *HRAS* (NC_000011), *KRAS* (NC_000012) and *NRAS* (NC_000001), in genomic DNA from 43 individuals with CFC syndrome (**Supplementary Methods** online). We identified two *KRAS* mutations: G60R (178G→C) in CFC73 and D153V (458A→T) in CFC8 and CFC91 (**Fig. 1a** and **Table 1**). Neither mutation has been previously identified in individuals with cancer (Sanger Institute Catalogue of Somatic Mutations in Cancer (COSMIC); http://www.sanger.ac.uk/cosmic). Gly60 and Asp154 are evolutionally conserved or chemically similar (**Supplementary Fig. 1** online). Neither of the two mutations was observed in 100 control chromosomes (data not shown). Their parents did not carry the mutations (**Supplementary Fig. 1**). The D153V mutation was identified in DNA extracted from both blood and buccal cells of individual CFC91. These results suggest that these germline mutations occurred *de novo*. No mutations in *KRAS*, *NRAS* or *HRAS* were found in the other 40 individuals with CFC syndrome.

Next, we examined the downstream molecules of RAS in the signaling pathway. The *RAF* proto-oncogene family consists of three isoforms, *CRAF*, *BRAF* and *ARAF*, and encodes for cytoplasmic serine/threonine kinases that are activated by binding RAS. Among these RAF molecules, BRAF is expressed at high levels in the brain and mutations in *BRAF* have been identified in 7% of all cancers[9]. We sequenced the entire 18 coding exons of *BRAF* (NC_000007) in 40 individuals with CFC syndrome and identified eight mutations in sixteen individuals (**Table 1**). Six mutations were located in the kinase domain (**Fig. 1b**). A G469E (1406G→A) mutation, which resides in the glycine-rich loop where somatic mutations are clustered in cancer, was identified in four individuals (CFC76, CFC81, CFC94 and CFC114). N581D (1741A→G), located in the catalytic loop, was identified in CFC95 and CFC110. Four mutations in the kinase domain between the glycine-rich loop and the catalytic loop were identified in five affected individuals: L485F (1455G→C) in CFC83, K499E (1495A→G) in CFC79, E501K (1501G→A) in CFC77 and E501G (1502A→G) in CFC90 and CFC105. A246P (736G→C) and

[1]Department of Medical Genetics, Tohoku University School of Medicine, Sendai, Japan. [2]Università Cattolica, Istituto di Genetica Medica, Rome, Italy. [3]Department of Genetics, Hôpital Robert Debré (APHP), Paris, France. [4]Department of Planning and Research, Osaka Medical Center and Research Institute for Maternal and Child Health, Izumi, Osaka, Japan. [5]Clinical and Molecular Genetics Unit, Institute of Child Health, London, UK and Department of Pediatrics, Academic Medical Center, Amsterdam, Netherlands. [6]Institut für Humangenetik, Universität Essen, Essen, Germany. [7]Medical Genetics Center, Federal University of Sao Paulo (UNIFESP), Sao Paulo, Brazil. [8]Division of Medical Genetics, Kanagawa Children's Medical Center, Yokohama, Japan. [9]Division of Medical Genetics, Saitama Children's Medical Center, Saitama, Japan. [10]Great Ormond Street Hospital, London, UK. [11]Genetic Department, Pitie-Salpetriere University Hospital, Paris, France. [12]Genetic Department, University Hospital, Angers, France. [13]Unità Operativa Complessa Patologia Neonatale e Terapia Intensiva, Dipartimento di Scienze Pediatriche Mediche e Chirurgiche, Azienda Ospedaliera Universitaria G. Martino, Messina, Italy. [14]Department of Medical Genetics, University of the Ryukyus School of Medicine, Okinawa, Japan. [15]Department of Human Genetics,Yokohama City University Graduate School of Medicine, Yokahama, Japan. [16]Comprehensive Research and Education Center for Planning of Drug Development and Clinical Evaluation, 21st Century COE Program, Tohoku University, Sendai, Japan. Correspondence should be addressed to Y.A. (aokiy@mail.tains.tohoku.ac.jp).

Received 20 November 2005; accepted 17 January 2006; published online 12 February 2006; doi:10.1038/ng1749

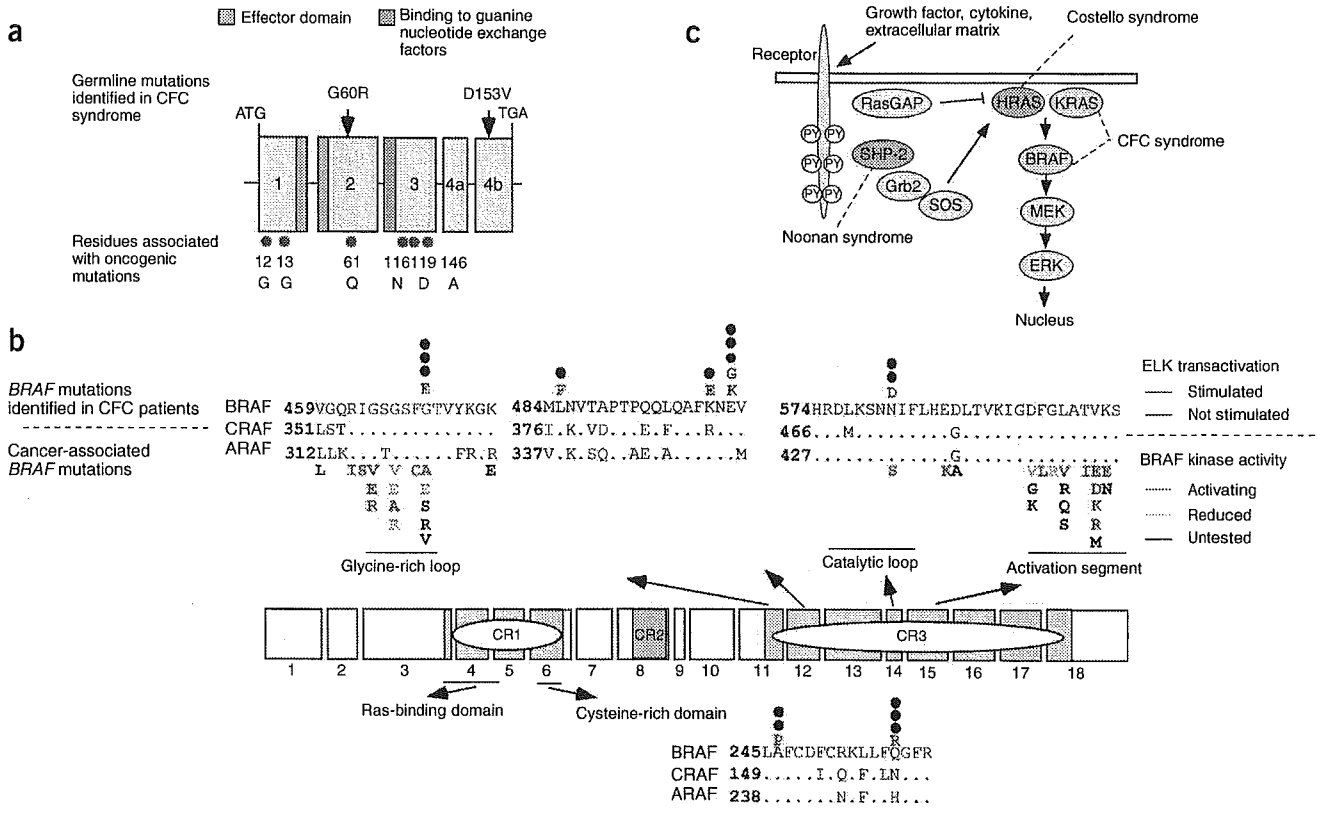

Figure 1 Mutations in *KRAS* and *BRAF* were identified in individuals with CFC syndrome. (**a**) Domain organization and genomic structure of the *KRAS* gene. Coding exons are numbered. In 98% of the transcripts, exon 4a is spliced out and only exon 4b is available for translation into protein. (**b**) *BRAF* consists of 18 exons. The three regions conserved in all RAF proteins (conserved region (CR) 1, CR2, and CR3) are shown in blue, green and yellow, respectively. The kinase domain is located in the CR3 domain. Six substitutions identified in CR3 are shown above. Filled circles indicate number of individuals having the substitution. Cancer-associated *BRAF* mutations are shown below the alignment of three RAF proteins[9,12]. Mutations detected in cancer are clustered in the glycine-rich loop and the activation segment of CR3 domain. The V600E mutation accounts for over 90% of the mutations in melanoma and thyroid cancer. Two mutations in the cysteine-rich domain were identified in five CFC individuals. Amino acids in CRAF and ARAF that are conserved in BRAF are shown by dots[13]. (**c**) RAS-ERK signaling pathway and associated disorders. RAS binds and stimulates RAF activation, which then activates MEK, which in turn activates ERK. ERK regulates gene expression and cytoskeletal rearrangements to coordinate the response to extracellular signals and regulate proliferation, differentiation, senescence and apoptosis[8,9]. Substitutions in *PTPN11*, *HRAS*, *KRAS* or *BRAF*, which potentially dysregulate the RAS-ERK signaling pathway, account for similar developmental disorders.

© 2006 Nature Publishing Group http://www.nature.com/naturegenetics

Q257R (770A→G), located in the cysteine-rich domain, were identified in five patients (**Fig. 1b** and **Table 1**). The identified eight substitutions were not found in 100 control chromosomes (data not shown). Mutation analysis in parents of five individuals (CFC76, CFC77, CFC96, CFC103 and CFC114) showed that these mutations occurred *de novo* (**Supplementary Fig. 2** online). The identified *BRAF* mutations were located in exons 6, 11, 12 and 14, and these domains were highly conserved in *CRAF* and *BRAF*. Sequencing of four corresponding exons in *CRAF*, ubiquitously expressed RAF, did not show any mutations in 24 individuals (data not shown).

KRAS and BRAF molecules are the key regulators of the RAS-RAF-MEK-ERK pathway, which is important for proliferation, growth and death of cells[9]. To elucidate critical steps, we examined the effect of the identified mutations on the RAS-ERK pathway by studying the activation of the ELK transcription factor. We transfected expression constructs (*KRAS* cDNA, NM_004985; *BRAF* cDNA, NM_00433) with a pFR-luc *trans*-reporter vector, a pFA2-ELK1 vector and a phRLnull-luc vector in NIH3T3 cells and determined their relative luciferase activity (RLA). We observed a significant increase in RLA in cells transfected with *KRAS* D153V but not in cells transfected with *KRAS* G60R (**Supplementary Fig. 3** online). We observed a two- to fourfold increase in RLA in cells transfected with two *BRAF* mutations (A246P and Q257R) in the cysteine-rich domain as well as in cells transfected with two *BRAF* mutations (L485S and K499E) in the kinase domain. We did not observe any significant increase in RLA in the other four mutations. Protein blotting showed that the wild-type and mutant proteins of *KRAS* and *BRAF* were equally expressed (data not shown). These results suggest that one *KRAS* and four *BRAF* mutants identified in CFC syndrome stimulated a common signaling pathway.

We identified substitutions of two proto-oncogenes, *KRAS* and *BRAF*, in 44% of individuals with CFC syndrome, suggesting that *KRAS* and *BRAF* have similar roles in human development. Controversy has existed as to whether CFC and Noonan syndromes are distinct disorders or different phenotypes of the same condition[2,10]. The clinical data of the 19 mutation-positive CFC individuals showed a high frequency of growth failure (78.9%), mental retardation (100%), relative macrocephaly (78.9%), characteristic facial appearance, including bitemporal constriction (84.2%) and downslanting palpebral fissures (94.7%), curly sparse hair (100%), heart defects (84.2%) and skin abnormalities (68.4%) (**Supplementary Table 1** online). This is in contrast with Noonan syndrome, in which there are lower frequencies of mental retardation (24–35%), heart defects (50–67%) and skin

Table 1 Mutations in 19 individuals with CFC syndrome

Individual	Gene	Exon	Nucleotide substitution	Amino acid change
CFC73	KRAS	2	178G→C	G60R
CFC8	KRAS	4b	458A→T	D153V
CFC91	KRAS	4b	458A→T	D153V
CFC100	BRAF	6	736G→C	A246P
CFC103	BRAF	6	736G→C	A246P
CFC16	BRAF	6	770A→G	Q257R
CFC24	BRAF	6	770A→G	Q257R
CFC96	BRAF	6	770A→G	Q257R
CFC76	BRAF	11	1406G→A	G469E
CFC81	BRAF	11	1406G→A	G469E
CFC94	BRAF	11	1406G→A	G469E
CFC114	BRAF	11	1406G→A	G469E
CFC83	BRAF	12	1455G→C	L485F
CFC79	BRAF	12	1495A→G	K499E
CFC77	BRAF	12	1501G→A	E501K
CFC90	BRAF	12	1502A→G	E501G
CFC105	BRAF	12	1502A→G	E501G
CFC95	BRAF	14	1741A→G	N581D
CFC110	BRAF	14	1741A→G	N581D

abnormalities (2–27%)[2]. Mutation analysis of *PTPN11* was negative in 43 CFC individuals. We did not identify any mutations in any exons of *KRAS* or in exons 6, 11, 12 and 14 of *BRAF* in 26 individuals with *PTPN11*-negative Noonan syndrome (data not shown), suggesting that Noonan syndrome and CFC syndrome are distinct clinical entities.

Comparison of manifestations between *KRAS*-positive and *BRAF*-positive individuals showed similar frequencies of growth and mental retardation, craniofacial appearance, abnormal hair and heart defects (**Supplementary Tables 2** and **3** online). However, we did observe a difference between the two groups in manifestations of skin abnormality, including ichthyosis, hyperkeratosis and hemangioma, which were observed in 13 *BRAF*-positive individuals. In contrast, no *KRAS*-positive individuals had these skin problems ($P < 0.05$). Somatic mutations in *BRAF* were identified in 60% of malignant melanoma or nevi[9], suggesting that BRAF has an important role in the skin. Comparison of manifestations between individuals with mutations that induced ELK transactivation and those with mutations that did not induce ELK transactivation showed no significant differences. Further analysis in a larger cohort would clarify the genotype-phenotype relationship in affected individuals.

The crystal structure of the BRAF kinase domain showed that the six *BRAF* mutations identified in this study are located in the interface of the ATP binding cleft, suggesting that these mutations may alter the catalytic activity of kinase domain (**Supplementary Fig. 4** online). Luciferase assays showed that two mutations (L485F and K499E) stimulated ELK-dependent transcription, suggesting that these mutants activated the ERK pathway. Missense mutations of *BRAF* were identified in approximately 7% of cancers, including human malignant melanoma and colorectal cancer[9]. The most frequent (>90%) V600E mutant showed elevated kinase activity, resulting in the activation of ERK and increased transformation activity[11]. Other less frequent mutations identified in cancer had either elevated or reduced kinase activity[9]. The four mutations identified in the kinase domain in our study did not enhance ELK-dependent transcription. This is in agreement with recent studies reporting that the activation of ERK or ELK transcription was not observed in cancer-associated mutations, including G469E (ref. 12). In cancer, *BRAF* mutations other than V600E are sometimes coincident with *RAS* mutations[9]. Other genetic background may contribute to the pathogenesis of CFC syndrome, although we did not detect any mutations in *KRAS*, *HRAS* or *NRAS* in *BRAF*-positive individuals. Further functional analysis of *BRAF* mutations will help elucidate the effects of these mutations on cell signaling.

The A246P and Q257R mutations are the first to be identified in the cysteine-rich domain in *BRAF*. This cysteine-rich domain is adjacent to the RAS-binding domain in conserved region 1 (ref. 13). A past study has suggested that the cysteine-rich domain of CRAF not only binds activated small GTPase RAS, but also inhibits basal catalytic RAF activity by direct or indirect interaction with the catalytic domain[14]. Our luciferase assay showed that these two mutations significantly activated ELK-dependent transcription, suggesting that they contribute to the activation of *BRAF*, leading to stimulation of the RAS-ERK pathway.

Previous clinical reports have shown that the association with cancers is rare in CFC syndrome[15]. This is in contrast with individuals with Costello syndrome, who have a higher risk of cancer, including rhabdomyosarcoma, ganglioneuroblastoma and bladder carcinoma[8]. It is of note that individual CFC94 with a *BRAF* G469E mutation had acute lymphoblastoid leukemia[15]. Careful observation of affected individuals would clarify the possible predisposition to hematopoietic malignancy in CFC syndrome as described in Noonan syndrome[4].

To the best of our knowledge, this is the first report of germline mutations in *KRAS* and *BRAF*. Our results suggest that mutations in human oncogenes (*HRAS*, *KRAS*, *BRAF* and *PTPN11*) that potentially dysregulate the RAS-MAPK pathway represent a common fundamental mechanism of related developmental disorders, namely, Noonan syndrome, Costello syndrome and CFC syndrome (**Fig. 1c**).

GenBank accession numbers. *KRAS* coding region, NC_000012; *HRAS* coding region, NC_000011; *NRAS* coding region, NC_000001; *BRAF*, NC_000007; *KRAS* cDNA, NM_004985; *BRAF* cDNA, NM_004333.

Note: Supplementary information is available on the Nature Genetics website.

ACKNOWLEDGMENTS

We wish to thank the individuals and their families who participated in this study and the doctors who referred the cases. The support of CFC International in facilitating the collection of patient samples is gratefully acknowledged. We are grateful to J. Miyazaki, Osaka University, for supplying the pCAGGS expression vector. This work was supported by Grants-in-Aid from the Ministry of Education, Culture, Sports, Science and Technology of Japan and Grants-in-Aid from the Ministry of Health, Labor, and Welfare of Japan.

COMPETING INTERESTS STATEMENT

The authors declare that they have no competing financial interests.

Published online at http://www.nature.com/naturegenetics
Reprints and permissions information is available online at http://npg.nature.com/reprintsandpermissions/

1. Reynolds, J.F. *et al. Am. J. Med. Genet.* **25**, 413–427 (1986).
2. Wieczorek, D., Majewski, F. & Gillessen-Kaesbach, G. *G. Clin. Genet.* **52**, 37–46 (1997).
3. van Eeghen, A.M., van Gelderen, I. & Hennekam, R.C. *Am. J. Med. Genet.* **82**, 187–193 (1999).
4. Tartaglia, M. & Gelb, B.D. *Eur. J. Med. Genet.* **48**, 81–96 (2005).
5. Ion, A. *et al. Hum. Genet.* **111**, 421–427 (2002).
6. Kavamura, M.I. *et al. Eur. J. Hum. Genet.* **11**, 64–68 (2003).
7. Musante, L. *et al. Eur. J. Hum. Genet.* **11**, 201–206 (2003).
8. Aoki, Y. *et al. Nat. Genet.* **37**, 1038–1040 (2005).
9. Garnett, M.J. & Marais, R. *Cancer Cell* **6**, 313–319 (2004).
10. Neri, G., Zollino, M. & Reynolds, J.F. *Am. J. Med. Genet.* **39**, 367–370 (1991).
11. Davies, H. *et al. Nature* **417**, 949–954 (2002).
12. Ikenoue, T. *et al. Cancer Res.* **64**, 3428–3435 (2004).
13. Mercer, K.E. & Pritchard, C.A. *Biochim. Biophys. Acta* **1653**, 25–40 (2003).
14. Winkler, D.G. *et al. J. Biol. Chem.* **273**, 21578–21584 (1998).
15. van Den Berg, H. & Hennekam, R.C. *J. Med. Genet.* **36**, 799–800 (1999).

© 2006 Nature Publishing Group http://www.nature.com/naturegenetics

BRAIN RESEARCH 1071 (2006) 24–33

available at www.sciencedirect.com

SCIENCE DIRECT®

www.elsevier.com/locate/brainres

BRAIN RESEARCH

Research Report

De novo and salvage pathways of DNA synthesis in primary cultured neurall stem cells

Kenichi Sato[a,b], *Junko Kanno*[a], *Teiji Tominaga*[b], *Yoichi Matsubara*[a,c], *Shigeo Kure*[a,c,*]

[a]*Department of Medical Genetics, Tohoku University School of Medicine, 1-1 Seiryo-machi, Aobaku, Sendai 980-8574, Japan*
[b]*Department of Neurosurgery, Tohoku University School of Medicine, Sendai, Japan*
[c]*Tohoku University 21st Century COE Program "Comprehensive Research and Education Center for Planning of Drug Development and Clinical Evaluation," Sendai, Japan*

ARTICLE INFO

Article history:
Accepted 6 November 2005
Available online 10 January 2006

Keywords:
Neural stem cell
Neurosphere
Proliferation
DNA synthesis pathway
Folic acid

ABSTRACT

We studied the de novo and salvage pathways of DNA synthesis in sphere-forming neural stem cells obtained from mouse embryos by a neurosphere method. The former pathway needs folic acid (FA) for nucleotide biosynthesis, while the latter requires deoxyribonucleosides (dNS). We examined the proliferative activity of sphere-forming cells in E14.5 embryos by counting the number of spheres formed in media that lacked FA and/or dNS. Proliferation failure and apoptosis occurred in a deficient medium lacking of both FA and dNS. Spheres formed in the deficient medium supplemented with dNS, without FA, did not produce neuron, but rather only seem to generate astrocytes and oligodendrocytes when plated under differentiation condition in culture. On the other hand, a subpopulation of cultured cells formed spheres in the deficient medium supplemented with FA alone in an appropriate concentration, and did possess the self-renewing and multipotential characteristics of neural stem cells. Spheres formed in the media containing low dose Azathioprine and methotrexate, inhibitors of de novo DNA synthesis, were selectively prevented from producing neurons even in the presence of FA. These results suggested that activating de novo DNA synthesis was needed for neural stem cells to proliferate with multipotentiality.

© 2005 Elsevier B.V. All rights reserved.

* *Corresponding author.* Department of Medical Genetics, Tohoku University School of Medicine, 1-1 Seiryo-machi, Aobaku, Sendai 980-8574, Japan. Fax: +81 22 717 8142.
E-mail address: skure@mail.tains.tohoku.ac.jp (S. Kure).

0006-8993/$ – see front matter © 2005 Elsevier B.V. All rights reserved.
doi:10.1016/j.brainres.2005.11.039

Abbreviations:
FA, folic acid
dNS, deoxyribonucleosides
dNTPs, deoxynucleoside triphosphates
dAdo, 2′-deoxyadenosine
dCyd, 2′-deoxycytidine
dGuo, 2′-deoxyguanosine
Thy, thymidine
AZP, azathioprine
MTX, methotrexate
NTD, neural tube defect
DIV, days in vitro
GFAP, glial fibrillary acidic protein

1. Introduction

Normal CNS development involves the sequential differentiation of multipotent stem cells. Alteration in the number of stem cells or their proliferative capability has major effects on the appropriate development of the nervous system (Sommer and Rao, 2002). One of the essential steps for the proliferation of stem cells is DNA synthesis. DNA precursors, i.e., nucleotides, are synthesized through two metabolic pathways referred to as de novo pathway and salvage pathway (Fig. 1). In the de novo pathway, deoxynucleoside triphosphates (dNTPs) are generated in multiple steps from 5-phosphoribosyl-1-pyrophosphate, glutamine, glycine, aspartate, and folic acid (FA). Since animal cells cannot synthesize FA, FA supplementation into their culture media is required for activating de novo DNA synthesis (Murray et al., 1999). In the salvage pathway, dNTPs are produced in single steps from exogenous and endogenous deoxyribonucleosides (dNS). The de novo pathway is predominant in normal differentiated tissues, whereas the salvage pathway is activated in rapidly proliferating tissues, including fetal and regenerative tissues and cancer cells (Hatse et al., 1999). Previous studies functionally evaluated the DNA synthesis in erythroblasts using culture media deficient of FA and/or dNS, and that indicated that erythroblasts underwent apoptosis during S phase in the lack of both FA and dNS (James et al., 1994; Koury and Horne, 1994; Koury et al., 2000). To date, the DNA synthesis pathway employed in neural stem cells remains uninvestigated.

Reynolds and Weiss (1996) reported that neural stem cells could be established from rodent brains by the neurosphere culture method. Using the neurosphere method, single

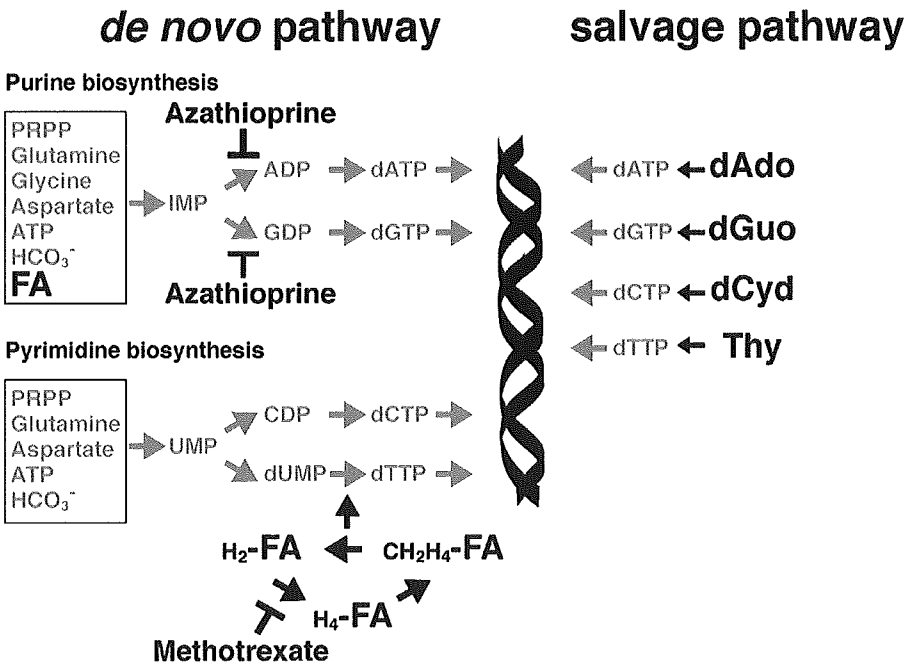

Fig. 1 – De novo and salvage biosynthesis of DNA. DNA is synthesized through two pathways: the de novo pathway (left panel) and salvage pathway (right panel). Abbreviations: IMP, inosinic acid; UMP, uridine monophosphate; dAdo, 2′-deoxyadenosine; dCyd, 2′-deoxycytidine; dGuo, 2′-deoxyguanosine; Thy, thymidine; H_2-FA, dihydrofolate; H_4-FA, tetrahydrofolate; CH_2H_4-FA, N^5,N^{10}-methylenetetrahydrofolate.

neural stem cells can be selectively expanded in a chemically defined medium containing epidermal growth factor (EGF), fibroblast growth factor 2 (FGF-2), or both, giving rise to floating spheroid cell aggregates called neurospheres. Since D-MEM/F-12, the commonly used medium for the neurosphere culture, contains both FA and two kinds of dNS, namely, thymidine (Thy) and hypoxanthine, the pathway of DNA synthesis that operates in the proliferation of neural stem cells remains unknown.

In this report, we performed the neurosphere method by using a custom-prepared D-MEM/F-12 medium that lacked FA and/or dNS for the functional evaluation of DNA synthesis pathways in embryonic sphere-forming neural stem cells. We examined the efficiency of the sphere formation and characterized the multipotency of the neural stem cells by in vitro differentiation analysis. Specific inhibitors of de novo DNA synthesis were used for the further characterization of sphere-forming cells. These approaches enabled us, for the first time, to perform the functional evaluation of DNA synthesis in neural stem cells.

2. Results

2.1. *Sphere formation derived from the E14.5 mouse striata in FA+/dNS− or FA−/dNS+ media*

To determine the DNA synthesis pathway utilized by embryonic neural stem cells for proliferation, we cultured neurospheres derived from the E14.5 mouse striata in D-MEM/F-12 medium lacking the precursors of DNA synthesis, defined as a deficient medium. We supplemented the deficient medium with varying amounts of FA, as a precursor for the de novo pathway, or dNS (equimolar addition of dAdo, dGuo, dCyd, and Thy), as precursors for the salvage pathway. In the deficient medium, designated as FA−/dNS− medium, no sphere was formed, and the condensation of cultured cells and the fragmentation of nuclei, which are characteristic of apoptosis, were observed. Terminal deoxynucleotidyl transferase-mediated dUTP-biotin nick end labeling (TUNEL) showed increased TUNEL-positive cells (mean ± SEM, 56.7% ± 1.5%; $n = 4$) in the deficient medium when compared with those in the deficient medium containing 10 μM FA and 50 μM dNS (29.2% ± 1.1%, $n = 5$, $P < 0.01$) (data not shown). These results suggested that cultured cells did not proliferate and underwent apoptosis in the medium without the precursors of DNA synthesis. In the medium containing only FA, maximum number of spheres was formed with 10 μM FA (Fig. 2A). In the absence of FA, peak sphere formation efficiency with each dNS was observed at a concentration of 50 μM (Fig. 2B). We defined the culture condition of 10 μM FA without dNS as FA+/dNS−. Similarly, the condition in which the culture was supplemented with 50 μM of each dNS without FA was designated as FA−/dNS+.

2.2. *Sphere-forming activity in the presence of various combinations of dNS*

Eukaryotes generally have converting enzymes among purine and pyrimidine deoxyribonucleosides (Murray et al., 1999). To determine the precursors of the salvage pathway that are required for sphere formation, we tested 16 different combinations of 10 μM dNS. As shown in Fig. 2C, the combination of dAdo with Thy yielded maximum sphere-forming efficiency and additional supplementation with other dNSs had little effect on the efficiency.

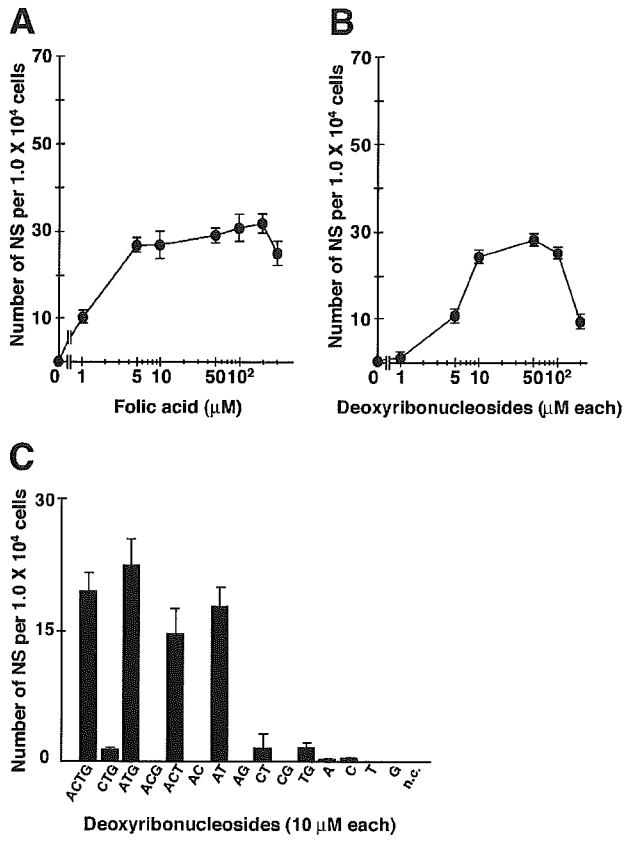

Fig. 2 – (A and B) Dose–response curves of sphere formation cultured for 7 DIV in the deficient medium supplemented with FA (A) or dNS (B). During this developmental period, spheres can be formed in the presence of FA or dNS in an appropriate concentration. (C) The number of spheres cultured for 7 DIV in the deficient medium supplemented with 16 different combinations of deoxyribonucleosides, each at a concentration of 10 μM. Graphs show mean ± SEM number of spheres per 1 × 10^4 cells prepared from the E14.5 mouse striata. Abbreviations: A, 2′-deoxyadenosine; C, 2′-deoxycytidine; G, 2′-deoxyguanosine; T, thymidine.

2.3. *Developmental-stage specific changes of sphere-forming activities under the FA+/dNS− and FA−/dNS+ conditions*

To examine the developmental changes of sphere-forming activities under the FA+/dNS− and FA−/dNS+ conditions, we performed the neurosphere cultures derived from the E12.5 and E16.5 mice striata in the deficient medium supplemented with varying amounts of FA or dNS (Fig. 3). In the cultures derived from the E16.5 striata, nearly the same number of spheres was formed with appropriate concentrations of FA and dNS. However, in the culture derived from

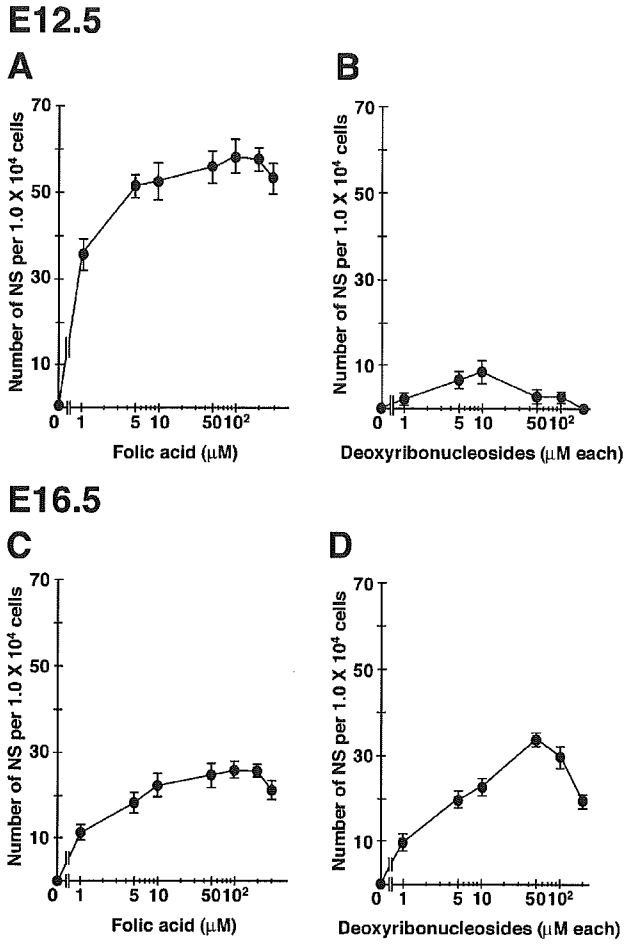

Fig. 3 – Developmental change of dose–response curve of sphere formation, cultured for 7 DIV in the deficient medium supplemented with FA (A and C) or dNS (B and D). Graphs show mean ± SEM number of spheres per 1 × 10^4 cells prepared from E12.5 (A and B) and E16.5 (C and D) mice striata.

E12.5, only a few spheres were formed under the FA–/dNS+ condition.

2.4. *Morphological and immunochemical characterizations of the formed spheres in the FA+/dNS– or FA–/dNS+ media*

Spheres formed under the FA–/dNS+ condition morphologically differed from those formed under the FA+/dNS– condition (Figs. 4A, B). After 7 DIV, the FA+/dNS– spheres were large, smooth, and spherical in shape, while the FA–/dNS+ spheres were small and irregular in shape. The FA+/dNS– spheres were 77.0 ± 3.8 μm (n = 66) in diameter, larger than the FA–/dNS+ spheres (49.8 ± 2.5 μm, n = 78, $P < 0.01$). It is unlikely that both spheres were derived from ciliated cells by their morphological characteristics (Chiasson et al., 1999; Laywell et al., 2000). Immunochemical characterization showed that both spheres were immunopositive for Nestin (a neural progenitor marker), GFAP (an astrocyte marker), and O4 (an oligodendrocyte marker) (Figs. 4C, D, G–J). However, tubulin β III (a neuron marker) positive cells were observed only in the FA+/dNS– spheres (Fig. 4E), and not in the FA–/dNS+ spheres (Fig. 4F), suggesting that cells in the FA–/dNS+ spheres barely differentiated into neurons.

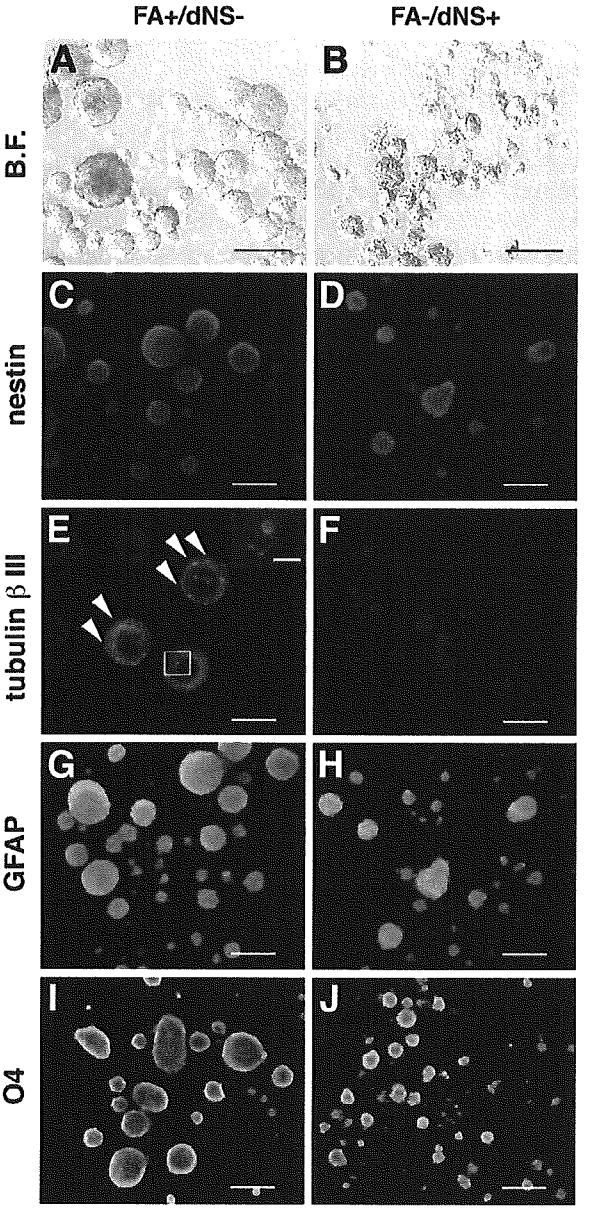

Fig. 4 – FA–/dNS+ spheres contain astrocytes and oligodendrocytes, but not neurons. (A and B) Phase-contrast images of live floating spheres under the FA+/dNS condition (A) and FA–/dNS+ condition (B). (C–J) Immunofluorescence of chemical markers for neural progenitors (nestin, red; C and D), neurons (tubulin β III, red; E and F), astrocytes (GFAP, green; G and H), oligodendrocytes (O4, green; I and J), and nucleus (DAPI, *blue; C–J*) derived from the FA+/dNS– spheres (C, E, G, and I) and FA–/dNS+ spheres (D, F, H, and J). White arrowheads indicate tubulin β III-positive neurons. Inset in panel E is high magnification of a white box. Scale bars: A–J, 200 μm; Inset, 20 μm. Abbreviations: B.F., bright field; GFAP, glial fibrillary acidic protein.